bioRxiv preprint doi: https://doi.org/10.1101/2022.06.14.496062; this version posted June 15, 2022. The copyright holder for this preprint (which was not certified by peer review) is the author/funder, who has granted bioRxiv a license to display the preprint in perpetuity. It is made available under aCC-BY 4.0 International license.

HIV skews the SARS-CoV-2 B cell response toward an extrafollicular maturation pathway

Robert Krause[1,2], Jumari Snyman[1,2,3], Hwa Shi-Hsia[1,5], Daniel Muema[1,2,3], Farina Karim[1,2], Yashica Ganga[1], Abigail Ngoepe[1], Yenzekile Zungu[1,2], Inbal Gazy[2,4], Mallory Bernstein[1], Khadija Khan[1,2], Matilda Mazibuko[1], Ntombifuthi Mthabela[1], Dirhona Ramjit[1], COMMIT-KZN Team, Oliver Limbo[6], Joseph Jardine[6], Devin Sok[6], Ian Wilson[7], Willem Hanekom[1,5], Alex Sigal[1,2,8,9], Henrik Kloverpris[1,5,10], Thumbi Ndung'u[1,2,3,5,8], Alasdair Leslie[1,5]

[1]Africa Health Research Institute, KwaZulu-Natal, South Africa

[2]School of Laboratory Medicine and Medical Sciences, University of KwaZulu-Natal, Durban, South Africa

[3]HIV Pathogenesis Programme, The Doris Duke Medical Research Institute, University of KwaZulu-Natal, Durban, South Africa

[4]KwaZulu-Natal Research Innovation and Sequencing Platform, Durban 4001, South Africa

[5]Division of Infection and Immunity, University College London, London, UK

[6]International AIDS Vaccine Initiative, NY, USA

[7]The Scripps Research Institute, La Jolla, CA, USA

[8]Max Planck Institute for Infection Biology, Berlin, Germany

[9]Centre for the AIDS Programme of Research in South Africa, Durban, South Africa

[10]Department of Immunology and Microbiology, University of Copenhagen, Copenhagen, Denmark

Background:

HIV infection dysregulates the B cell compartment, affecting memory B cell formation and the antibody response to infection and vaccination. Understanding the B cell response to SARS-CoV-2 in people living with HIV (PLWH) may explain the increased morbidity, reduced vaccine efficacy, reduced clearance, and intra-host evolution of SARS-CoV-2 observed in some HIV-1 coinfections.

Methods:

We compared B cell responses to COVID-19 in PLWH and HIV negative (HIV-ve) patients in a cohort recruited in Durban, South Africa, during the first pandemic wave in July 2020 using detailed flow cytometry phenotyping of longitudinal samples with markers of B cell maturation, homing and regulatory features.

Results:

This revealed a coordinated B cell response to COVID-19 that differed significantly between HIV-ve and PLWH. Memory B cells in PLWH displayed evidence of reduced germinal center (GC) activity, homing capacity and class-switching responses, with increased PD-L1 expression, and decreased Tfh frequency. This was mirrored by increased extrafollicular (EF) activity, with dynamic changes in activated double negative (DN2) and activated naïve B cells, which correlated with anti-RBD-titres in these individuals. An elevated SARS-CoV-2 specific EF response in PLWH was confirmed using viral spike and RBD bait proteins.

bioRxiv preprint doi: https://doi.org/10.1101/2022.06.14.496062; this version posted June 15, 2022. The copyright holder for this preprint (which was not certified by peer review) is the author/funder, who has granted bioRxiv a license to display the preprint in perpetuity. It is made available under aCC-BY 4.0 International license.

Conclusions:

Despite similar disease severity, these trends were highest in participants with uncontrolled HIV, implicating HIV in driving these changes. EF B cell responses are rapid but give rise to lower affinity antibodies, less durable long-term memory, and reduced capacity to adapt to new variants. Further work is needed to determine the long-term effects of HIV on SARS-CoV-2 immunity, particularly as new variants emerge.

Funding:

This work was supported by a grant from the Wellcome Trust to the Africa Health Research Institute (Wellcome Trust Strategic Core Award [grant number 201433/Z/16/Z]). Additional funding was received from the South African Department of Science and Innovation through the National Research Foundation (South African Research Chairs Initiative, [grant number 64809]), and the Victor Daitz Foundation.

Introduction

SARS-CoV-2 remains a threat to global health, especially in the light of new, more contagious variants capable of escaping vaccine-induced neutralizing antibodies (Cele et al., 2021; Tada et al., 2021; Tegally et al., 2021; Wibmer et al., 2021). Although vaccination may not prevent transmission, it is generally effective at preventing severe disease, primarily via eliciting neutralizing antibodies targeting the SARS-CoV-2 spike protein (Frater et al., 2021; Shinde et al., 2021; Tada et al., 2021). Risk factors for severe disease, especially in unvaccinated people, include old age (>65), underlying lung and heart disease; diabetes; and immune disorders such as those caused by HIV infection (Williamson et al., 2020). HIV has also been associated with increased morbidity and mortality (Bhaskaran et al., 2021; Western Cape Department of Health in collaboration with the National Institute for Communicable Diseases, 2021), especially in patients with uncontrolled HIV viremia (Chanda et al., 2021) and in those with CD4 counts below 200 cells/µl, emphasizing the need for effective antiretroviral therapy (ART) (Karim et al., 2021). In addition, an inadequate immune response to COVID-19 is associated with prolonged SARS-CoV-2 infection and high intra-host mutation rates in both uncontrolled HIV and patients on immune-suppressing medication (Cele et al., 2022; McCormick, Jacobs, & Mellors, 2021). This highlights the importance of understanding the immune response to COVID-19 in patients with HIV, especially in the South African context, which has a high HIV prevalence (Kharsany et al., 2018) and SARS-CoV-2 attack rate (Tegally et al., 2021).

HIV affects the adaptive immune response by infecting CD4 T cells and reducing their numbers in circulation (Dalgleish et al., 1984; Westendorp et al., 1995). CD4 T follicular helper (Tfh) cells are a critical component of the germinal center (GC) reaction as they assist the affinity maturation of their cognate B cell's antigen receptor (BCR). The knock-on effects of HIV infection can therefore include hypergammaglobulinemia (Lane et al., 1983), depleted resting memory, and increased naïve B cell frequencies (Moir & Fauci, 2014). Interestingly, as with other inflammatory diseases (Freudenhammer, Voll, Binder, Keller, & Warnatz, 2020), HIV is also associated with an increased prevalence of "tissue-like" memory B cells in circulation (Ehrhardt et al., 2005; Knox et al., 2017; Moir & Fauci, 2014). These CD27-ve CD21-ve B cells resemble the EF constituent now often referred to as double-negative (DN) B cells (Jenks, Cashman, Woodruff, Lee, & Sanz, 2019; Jenks et al., 2020; Woodruff et al., 2020). These HIV induced changes in the B cell compartment are likely to be responsible for the reduced vaccine efficacy and durability observed in PLWH, including to novel SARS-CoV-2 vaccines (Hassold et al., 2022; Kerneis et al., 2014), and may contribute to prolonged viremia and increased viral mutation (Cele et al., 2022; Karim et al., 2021).

bioRxiv preprint doi: https://doi.org/10.1101/2022.06.14.496062; this version posted June 15, 2022. The copyright holder for this preprint (which was not certified by peer review) is the author/funder, who has granted bioRxiv a license to display the preprint in perpetuity. It is made available under aCC-BY 4.0 International license.

We, therefore, investigated the effect of HIV on the B cell response to SARS-CoV-2 infection, using a comprehensive B cell phenotyping approach and B cell baits to identify SARS-CoV-2 specific B cells. Blood samples were collected at weekly intervals from PLWH and HIV-ve study participants following positive COVID-19 diagnosis during the first wave of infections in a cohort of patients from Durban, South Africa (Karim et al., 2021). In this cohort of individuals with predominantly mild-moderate disease, the B cell response to SARS-CoV-2 infection is strikingly different in PLWH and characterized by reduced GC activity and a contrasting increase in EF activity.

Results

We investigated the longitudinal dynamics of the B cell response to SARS-CoV-2 infection in PLWH compared to HIV-ve patients using a previously described COVID-19 cohort enrolled in Durban, South Africa, during the first wave of the pandemic in July 2020 (Karim et al., 2021). A total of 70 SARS-CoV-2 positive, confirmed by qPCR and serology, and 10 negative control participants were included in this study. Of the SARS-CoV-2 positive participants, 28 (40%) were PLWH, and five (18%) had detectable HIV in their plasma. SARS-CoV-2 infected participants were monitored weekly for 5 follow-up time points. Control participants were recruited at a single time point and were confirmed as SARS-CoV-2 negative by qPCR and serology and included two PLWH individuals. As some of the participants remained asymptomatic throughout the study, a timescale relating to days after positive diagnostic swab rather than symptom onset was used (days post-diagnostic swab), which has been shown to correlate well with symptom onset in the symptomatic patients from this cohort (Karim et al., 2021).

B cells were initially identified as CD19+ lymphocytes (**Figure 1A**), and the expression pattern of CD27 and CD38 was used to identify the canonical naïve, memory, and antibody-secreting cell (ASC) subsets (Glass et al., 2020). The ASC population was further differentiated into CD138+ Plasma cells (PC) and CD138- Plasmablasts (PB) (Glass et al., 2020). Considering all timepoints, HIV viremic participants had lower absolute B cell numbers, although this difference did not reach statistical significance. However, HIV-ve SARS-CoV-2 infected participants had significantly fewer naïve B cells and more memory B cells than SARS-CoV-2 infected PLWH and SARS-CoV-2 uninfected controls (**Figure 1B;** (Moir & Fauci, 2014)). The ASC response was significantly elevated at SARS-CoV-2 viremic timepoints in both patient groups, consistent with a robust ASC response to active infection (**Figure 1C**) but was not significantly different in PLWH. In addition, although the frequency of ASC at the earliest timepoint tended to be higher in the HIV-ve group, this was not statistically significant. Using the patient neutrophil-lymphocyte ratio (NLR) as a proxy of inflammation (Ciccullo et al., 2020; Fu et al., 2020; Karim et al., 2021), the frequency of ASC was found to be significantly higher at time points when the NLR ratio was above 3 (**Figure 1D**) suggesting an association between disease severity and ASC frequency. Finally, the PC:PB ratio was not significantly different between PLWH and HIV-ve patients at any time point, although there was a trend for a lower ratio in PLWH (**Figure 1E**). Taken together these data suggest that despite differences in canonical B cell phenotypes known to precede ASC maturation, PLWH mounted a similar ASC response against SARS-CoV-2 infection to HIV-ve participants.

To further investigate the B cell response to SARS-CoV-2 in PLWH, we designed three B cell phenotyping flow cytometry panels, using markers specific for B cell maturation, activation, homing, and regulatory function (**Figure 2A, C, D**). Fresh PBMC from all participants were stained using all three panels separately and analyzed using an unbiased approach combining FlowSOM and tSNE pipelines (van der Maaten L., 2008; Van Gassen et al., 2015). This identified 11 to 12 distinct B cell clusters between the three phenotyping panels, with probable B cell phenotypes assigned based on the expression pattern of surface markers associated with each B cell cluster (**Figure 2A, C, D**). To uncover associations between HIV infection status or disease severity, an equal number of B cells for each disease severity category (ordinal scale 1-3 (OS1-3, (Karim et al., 2021)) were included, distributed

bioRxiv preprint doi: https://doi.org/10.1101/2022.06.14.496062; this version posted June 15, 2022. The copyright holder for this preprint (which was not certified by peer review) is the author/funder, who has granted bioRxiv a license to display the preprint in perpetuity. It is made available under aCC-BY 4.0 International license.

equally between PLWH and HIV-ve controls. This allowed the relative abundance of each B cell cluster to be compared between the following clinical parameters: an ordinal disease scale (1-3), neutrophil-lymphocyte ratio (NLR) as a measure of inflammation (Ciccullo et al., 2020; Fu et al., 2020; Karim et al., 2021), SARS-CoV-2 viral load and HIV status.

Using B cell panel 1 (**Extended Data Table 1, Figure 2A**), distinct patterns of homing marker expression were observed. Two CD27+CD38++ ASC populations are identified, highlighted in red and purple (**Figure 2A**). The former also expressed high levels of CXCR3, the primary receptor for CXCL9, 10, 11, which facilitates homing to inflamed tissues (Onodera et al., 2012; Serre et al., 2012; Sutton et al., 2021), high levels of the extravasation marker CD62L+ and, uniquely, the activation/tissue residency marker CD69+. Therefore, this population is referred to as tissue homing and potentially indicates B cells which preferentially migrate to the diseased lung (Onodera et al., 2012; Serre et al., 2012; Sutton et al., 2021; Weisel et al., 2020). In line with this, tissue homing ASC are highly elevated in participants with the most severe disease (ordinal scale 3), with elevated NLR, and with detectable SARS-CoV-2 viremia, as, to a lesser extent, are ASCs lacking this tissue homing phenotype (**Figure 2A, B**). In addition, a population of class switched, IgM^{hi} B cells (highlighted in blue) was associated with severe disease, which co-expressed markers associated with germinal center homing (CXCR5 and CXCR4; (Cyster & Allen, 2019)). Strikingly, all 3 populations are elevated in HIV-ve participants but not in PLWH, as indicated in the final 2 columns of the heat map. In PLWH, by contrast, disease severity was associated with an elevated population of B cells expressing a CD27-IgD- phenotype, corresponding to double negative B cells (DN; highlighted in grey), which lacked elevated expression of any of the homing markers measured. Several B cell subsets are elevated in asymptomatic subjects, including transitional B cells, as reported elsewhere (Woodruff et al., 2020) and a class-switched memory phenotype that expressed CXCR3. As expected, in the control patients, the naïve B cell phenotype was predominantly IgD+ IgM- (brown), whereas the SARS-CoV-2 infected participants IgD + naïve cells also expressed low levels of IgM+ (yellow; **Figure 2B**). Both naïve populations are high for CXCR5 and CXCR4, consistent with their requirement to gain entry to germinal centers for affinity maturation (dark and light zones, respectively (Cyster & Allen, 2019)). Interestingly CCR6 was also upregulated in the SARS-CoV-2+ naïve B cells, suggestive of systemic B cell activation (Reimer et al., 2017; Wiede et al., 2013). Together these data confirm that, as reported elsewhere (Woodruff et al., 2020), COVID-19 severity is associated with skewing of B cell phenotype and, for the first time, that this skewing is altered by concurrent HIV infection.

The association between disease severity and B cell phenotype was less apparent in data generated using the other two flow cytometry panels and, therefore not reported in the heat maps (**Figure 2C,D; Extended Data Figure 2B,C**). However, distinct differences between PLHW and HIV-ve participants were also apparent. Panel 2, composed of maturation markers (**Figure 2C**), again suggests that ASC were less prevalent in PLWH than in HIV-ve participants, particularly CD138+ plasma cells. In addition, class-switched memory cells (CSM) expressing CD69, consistent with activation, were elevated in HIV-ve participants but not PLWH. In contrast, two DN populations can be distinguished, differing by CD40 expression (purple and turquoise), both of which feed into an EF B cell maturation pathway (Jenks et al., 2019; Jenks et al., 2020; Woodruff et al., 2020), and both were elevated in PLWH. Likewise, an activated naïve ($CD21^{lo}$) population (orange) was also elevated in PLWH relative to HIV-ve participants. Two other naïve phenotypes were apparent, differing by their expression of CD40, of which the CD40-ve population appeared to be unique to the HIV-ve COVID-19+ participants (red population). Finally, two small transitional B cell populations were detectable, one of which, with a distinctive high IgD, CD21, and CD40 phenotype, was elevated in PLWH.

bioRxiv preprint doi: https://doi.org/10.1101/2022.06.14.496062; this version posted June 15, 2022. The copyright holder for this preprint (which was not certified by peer review) is the author/funder, who has granted bioRxiv a license to display the preprint in perpetuity. It is made available under aCC-BY 4.0 International license.

For panel 3, comprised of regulatory markers, the same reduced ASC response in PLWH was suggested (highlighted in blue), as the key B cell markers CD19, IgD, IgM, CD27, and CD38 are shared between all three panels. In this case, ASC are shown to express high levels of CD86, associated with B cell activation (Cyster & Allen, 2019). The same association between PLWH and DN B cells was also apparent (highlighted in orange), and which also display CD86 expression (**Figure 2D**). In addition, a small population of B cells expressing high levels of CD5 (CD5++) was elevated in PLWH. These cells co-express CD1d, consistent with regulatory B cells producing the critical regulatory cytokine IL-10 (Oleinika et al., 2018; Palmer, Nganga, Rothermund, Perry, & Swanson, 2015; Yanaba et al., 2008). Another important regulatory molecule in B cells is PD-L1, which can limit T-cell help via engaging with PD-1 on the surface of Tfh cells in the GC (Khan et al., 2015). The expression of this marker was primarily associated with B cell subsets present in non-COVID-19 controls (**Figure 2D**, pink and grey), suggesting it is downregulated during SARS-CoV-2 infection. However, PD-L1 expression did not appear to be affected by HIV coinfection. Taken together, these unbiased analyses consistently show the B cell response to SARS-CoV-2 is skewed in PLWH, associated with a reduction in ASC subsets, class switching, and markers of GC homing and with an increase of B cell phenotypes associated with EF maturation.

To drill down further, we next analyzed the skewed B cell subsets of interest in longitudinal samples by Boolean gating. Unlike in the tSNE analysis, where downsampling was used to prevent bias analysis, all study subjects were included in these analyses. Consistent with the potential difference in GC activity and class switching observed above, we found that CD27+ IgD- switched memory B cells (SM) were significantly more frequent in HIV-ve COVID-19 patients than in PLWH (**Figure 3A**). Furthermore, the fraction of SM B cells expressing CD62L and CXCR5, allowing them to home the GC, was reduced in PLWH, particularly in individuals with viremic HIV (**Figure 3B**). Longitudinal analysis shows this population increases over time in both groups, consistent with a dynamic change associated with SARS-CoV-2 infection but is consistently lower in PLWH (**Figure 3B**). A similar trend was observed for CSM B cells, which were expanded in HIV-ve participants compared to controls but were significantly lower in viremic PLWH (**Figure 3C**). Interestingly, IgM switched memory B cells were significantly upregulated in all COVID-19 patient groups relative to the control group, but again this was reduced in the PLWH group. Although the precise function of this B cell subset is debated, it is believed they can achieve rapid plasma cell differentiation, germinal center re-initiation, and IgM and IgG memory pool replenishment (Weill & Reynaud, 2020). Together these data suggest that concurrent HIV infection may cause a reduction in GC homing, class switching, and memory establishment after SARS-CoV-2 infection, which was generally exacerbated in individuals with viremic HIV.

Next, given that the alternative to B cell maturation in the GC involves an EF route, DN B cells were examined in detail. The DN phenotype, also referred to as atypical B cells, forms part of an EF B cell response, which circumvents/pre-empts the germinal center reaction resulting in a rapid but short-lived PB response that facilitates rapid antibody production (Jenks et al., 2019; Jenks et al., 2020; Woodruff et al., 2020). Both activated DN B cells, commonly referred to as the DN2 cells, and activated naïve phenotypes, contribute to the EF response (Jenks et al., 2019) and are identified as $CD21^{lo}$ CD95+ subsets (**Figure 4A**). Multiple studies have described the expansion of DN2 B cells in association with severe COVID disease (Chen et al., 2020; Kaneko et al., 2020; Woodruff et al., 2020), but not in relation to HIV. Here, DN2 and activated naïve B cells were identified by expression of CD95, a known marker of activation on B cells (Freudenhammer et al., 2020; Glass et al., 2020; Jenks et al., 2020; Le Gallo, Poissonnier, Blanco, & Legembre, 2017). Both EF-associated B cell phenotypes were significantly more frequent in the SARS-CoV-2 infected PLWH relative to the HIV-ve group, irrespective of HIV viremia in the case of DN2 (**Figure 4B and extended Figure 4A(i)**). In addition, both subsets change in frequency over the course of infection, expanding from timepoint 2 (day 7-13) and remaining significantly

bioRxiv preprint doi: https://doi.org/10.1101/2022.06.14.496062; this version posted June 15, 2022. The copyright holder for this preprint (which was not certified by peer review) is the author/funder, who has granted bioRxiv a license to display the preprint in perpetuity. It is made available under aCC-BY 4.0 International license.

expanded compared to HIV-ve participants until after timepoint 4 (day 21-27), after which they contract to the same level (**Figure 4C and extended Figure 4B**). The dynamic nature of this EF response strongly suggests it emerges during SARS-CoV-2 infection and does not represent a pre-existing difference associated with HIV. This is further supported by the fact that the frequency of DN2 and, to a lesser extent, activated naïve B cells, correlates with the RBD antibody titer in PLWH, particularly those with detectable HIV (**Figure 4D and extended Figure 4C**). In addition, the frequency of these populations was associated with increased clinical disease severity and NLR in PLWH but not in HIV-ve participants (**Figure 4C and extended Figure 4B**). Indeed, the lack of an EF response in HIV-ve participants is highlighted by the absence of DN populations even in subjects in OS3 and with elevated NLRs. These data are highly consistent with the data shown in **Figure 3** and suggest that the B cell response to SARS-CoV-2 infection in PLWH is associated with reduced GC maturation and increased EF activity.

Having observed elevated PD-L1 in non-COVID controls, we examined the expression of this marker longitudinally in conjunction with CD5 to examine regulatory B cell frequency (**Figure 5A;** (Catalan et al., 2021; Khan et al., 2015; Sun, Zhang, Li, Yin, & Xue, 2019). This revealed a clear shift in PD-L1 expression on naïve B cells longitudinally, which was very low at baseline and increased to the range observed in controls by the final time point (**Figure 5B**). Similar frequencies and longitudinal trends were observed in both PLWH and HIV-ve participants, suggesting this is a consistent feature of the acute B cell response to SARS-CoV-2 infection. However, PD-L1 CD5+ B cells are significantly more frequent in HIV viremic individuals (**Figure 4A)**. PD-L1 expression plays an integral part in the GC response and maintains the relatively unstable Tfh lineage (Khan et al., 2015). Interestingly, the frequency of total Tfh tended to be higher in PLWH, reaching significance at timepoints 2 and 5 (**Figure 4C**). Although the frequency of SARS-CoV-2 specific Tfh was not measured, these data again point to potential impairment of the GC response in PLWH, which is dependent on the crosstalk between B cells and Tfh governed, in part, by the interaction between PD-L1 expressed on B cells and PD-1 on Tfh (Khan et al., 2015; Sun et al., 2019).

Finally, as the data presented above was based on bulk B cell phenotyping, we examined a subset of informative markers on SARS-CoV-2 specific B cells using recombinant SARS-CoV-2 spike and receptor binding domain (RBD) proteins conjugated to fluorescent streptavidin as baits ((Goel et al., 2021) Krause et al., submitted; **Figure 6A; Extended Data Table 2**). B cells staining with both spike and RBD baits were quantified at baseline and 3 months, revealing robust SARS-CoV-2 specific memory B cell populations in all individuals, which did not significantly wane by 3 months and were not different in frequency between PLHW and HIV-ve participants (**Figure 6B**). Interestingly, in this subset of participants, the degree of CSM was not significantly different between groups and tended to increase over time in both. However, spike-specific memory B cells from PLWH tended to express higher levels of CXCR3 (**Figure 6C**), particularly at month 3, a marker associated with homing to inflamed tissue (Onodera et al., 2012; Serre et al., 2012; Sutton et al., 2021). Finally, a significantly higher proportion of spike-specific B cells from PLWH displayed a DN2 phenotype, confirming the increased EF activity towards SARS-CoV-2 in these individuals suggested by the bulk phenotyping.

Discussion

Using longitudinal samples from the first wave of infection in South Africa, we found that HIV coinfection significantly impacted the B cell response to SARS-CoV-2. Overall, these data show that the B cell response in PLWH is skewed towards an EF route and away from GC maturation. This is demonstrated by several observations, including elevated DN2 and activated naïve B cells in PLWH, consistent with EF maturation; mirrored by reduced class switching of memory B cells and reduced expression of markers CXCR5 and CD62L allowing B cells to home to the GC. In addition, as an effective

bioRxiv preprint doi: https://doi.org/10.1101/2022.06.14.496062; this version posted June 15, 2022. The copyright holder for this preprint (which was not certified by peer review) is the author/funder, who has granted bioRxiv a license to display the preprint in perpetuity. It is made available under aCC-BY 4.0 International license.

GC reaction requires tight regulation of the Tfh response, observed differences in PD-L1 expression on B cells and Tfh frequency in PLWH are likely to hamper B cell maturation via this pathway. Importantly, the skewing toward EF B cell maturation in PLWH correlated with anti-RBD antibody titer in these individuals and was confirmed on SARS-CoV-2 spike-specific B cells.

Multiple studies have characterized the B cell response to COVID-19 in HIV-ve individuals and observed a positive correlation between disease severity and an elevated ASC response (Kaneko et al., 2020; Karim et al., 2021; Woodruff et al., 2020). Furthermore, an EF B cell response has been associated with severe COVID-19 and predicts poor clinical outcomes, and severe COVID-19 cases have been characterized by poor GC formation in secondary lymphoid organs (Chen et al., 2020; Kaneko et al., 2020; Woodruff et al., 2020). However, the impact of HIV coinfection on the B cell response and these associations is unknown. Here, we find that the ASC response is associated with disease severity in both HIV-ve participants and PLWH, although the effect appears more robust in HIV-ve participants. More detailed phenotyping of the ASC supports this, as CD138+ plasma cells and ASC with a tissue homing and activated phenotype (CXCR3+CD69+ in panel 1 and CD86+ in panel 2) were more strongly associated with SARS-CoV-2 infection in HIV-ve participants. In contrast, the association between disease severity and EF activity was uniquely observed in PLWH. The absence of EF activity in HIV-ve participants is not at odds with published literature, as no individuals with severe COVID-19 were included in this study (Kaneko et al., 2020; Woodruff et al., 2020). Therefore, the association between HIV and EF B cells is not driven by disease severity.

Although not previously observed for COVID-19, the skewing of B cells towards an EF response in PLWH makes biological sense. Both DN2 and activated naïve B cells mature via an EF pathway, independent of T cell help and in response to pro-inflammatory cytokines IFNγ, TNFa, and IL-21; and TLR 7 and 9 stimulation (Jenks et al., 2019; Jenks et al., 2020). HIV induces a pro-inflammatory state (Connolly, Riddler, & Rinaldo, 2005; Roff, Noon-Song, & Yamamoto, 2014), making B cells more prone to EF maturation; and HIV viremia is known to induce a DN2 response (Amu, Ruffin, Rethi, & Chiodi, 2013; Ferreira et al., 2013). This link may explain the association between DN2 frequency and inflammation in PLWH, as measured by the NLR ratio. On the other hand, since HIV depletes CD4 T cells, it also impairs germinal center (GC) activity, including BCR somatic hypermutation, class switching, and, ultimately, the ASC response (Okoye & Picker, 2013; Pallikkuth et al., 2012; Perreau et al., 2013), consistent with the trends observed. Likewise, HIV alters the B cell compartment by affecting the frequencies of naïve and memory B cells (Moir & Fauci, 2014), again agreeing with the differences in the frequency of naïve and memory B cells observed in this study.

The downstream consequence of skewed B cell maturation in PLWH is unclear from this study. However, the EF response relies primarily on the existing germline and memory BCR repertoire, whereas the GC response allows for honing of the BCR repertoire through somatic hypermutation and stringent affinity selection of BCR clones to generate high-affinity long term ASC and memory responses (Jenks et al., 2020; Kaneko et al., 2020). Therefore, the loss of GC B cell maturation could result in a less effective B cell response to infection in PLWH and potentially a greater susceptibility to infection by variants. (Sette & Crotty, 2021) demonstrated that the antibody response to COVID-19 parent strain derives from the germline B cell receptor (BCR) repertoire without the need for extensive hypermutation. This might explain why HIV status did not seem to affect the antibody response during the first wave of infections (Snyman et al., 2021). In contrast, the antibody response to the second wave of infections was affected by HIV status, with PLWH mounting less effective IgG responses to the Beta variant (Hwa, Snyman et al., submitted). Therefore, the skewed EF B cell response could explain the less effective response against new variants. Indeed, multiple studies have revealed B cell maturation and expanded somatic hypermutation months after primary infection in COVID-19

bioRxiv preprint doi: https://doi.org/10.1101/2022.06.14.496062; this version posted June 15, 2022. The copyright holder for this preprint (which was not certified by peer review) is the author/funder, who has granted bioRxiv a license to display the preprint in perpetuity. It is made available under aCC-BY 4.0 International license.

patients without HIV (Gaebler et al., 2021; Wang et al., 2021) and have highlighted the importance of antibody affinity maturation (Chen et al., 2020; Muecksch et al., 2021) and class switching (Zohar et al., 2020) to reduce disease severity and gain improved efficacy against new variants. This might also explain the lack of effective clearance of SARS-CoV-2 in HIV viremic individuals and might be a mechanism for intra-host evolution in patients with uncontrolled HIV (Cele et al., 2022). Further work is needed to understand how the skewed B cell response to natural infection impacts long-term memory and the ability to adapt to new viral variants. It will also be essential to understand the impact of vaccination on the B cell memory compartment.

Acknowledgements

COMMIT-KZN Team

Moherndran Archary, Department of Paediatrics and Child Health, University of KwaZulu-Natal; Kaylesh J. Dullabh, Department of Cardiothoracic Surgery, University of KwaZulu-Natal; Jennifer Giandhari, KwaZulu-Natal Research Innovation and Sequencing Platform; Philip Goulder, Africa Health Research Institute and Department of Paediatrics, Oxford; Guy Harling, Africa Health Research Institute and the Institute for Global Health, University College London; Rohen Harrichandparsad, Department of Neurosurgery, University of KwaZulu-Natal; Kobus Herbst, Africa Health Research Institute and the South African Population Research Infrastructure Network; Prakash Jeena, Department of Paediatrics and Child Health, University of KwaZulu-Natal; Thandeka Khoza, Africa Health Research Institute; Nigel Klein, Africa Health Research Institute and the Institute of Child Health, University College London; Rajhmun Madansein, Department of Cardiothoracic Surgery, University of KwaZulu-Natal; Mohlopheni Marakalala, Africa Health Research Institute and Division of Infection and Immunity, University College London; Mosa Moshabela, College of Health Sciences, University of KwaZulu-Natal; Kogie Naidoo, Centre for the AIDS Programme of Research in South Africa; Zaza Ndhlovu, Africa Health Research Institute and the Ragon Institute of MGH, MIT and Harvard; Kennedy Nyamande, Department of Pulmonology and Critical Care, University of KwaZulu-Natal; Nesri Padayatchi, Centre for the AIDS Programme of Research in South Africa; Vinod Patel, Department of Neurology, University of KwaZulu-Natal; Theresa Smit, Africa Health Research Institute; Adrie Steyn, Africa Health Research Institute and Division of Infectious Diseases, University of Alabama at Birmingham

Figure Legends

Figure 1. Canonical B cell phenotype frequencies vary with HIV status but still mount robust antibody secreting cell (ASC) responses. (**A**) Gating strategy to identify CD19+ B cells within the PBMC compartment. B cells were further gated on CD27 and CD38 to identify CD27+ Memory, CD27- Naïve and CD27+CD38++ ASC. (**B**) Absolute B cell counts were calculated from patient total lymphocyte counts, followed by percent Naïve, Memory and ASC fractions of the CD19+ parent population. (**C**) The ASC response associated with SARS-CoV-2 viremia and was tracked longitudinally up to day 35 post diagnosis. (**D**) A neutrophil lymphocyte ratio (NLR) served as a proxy of inflammation and associated with the ASC as well as Plasmablast and Plasma cell responses. Statistical analyses were performed using the Kruskal-Wallis H test for multiple comparisons and Mann-Whitney for SARS-CoV-2 viremia or NLR comparisons within groups. *P* values are denoted by * ≤ 0.05; ** < 0.01; *** < 0.001 and **** < 0.0001.

Figure 2. tSNE analysis of the B cell phenotypes and frequencies relative to COVID-19 clinical parameters including disease severity, neutrophil lymphocyte ratio, SARS-CoV-2 viremia, and HIV status. A total of 80000 CD19+ B cells from four patient groups (20000 cells per group) were used in an unbiased tSNE analysis. Patients were grouped by decreasing disease severity according to an

bioRxiv preprint doi: https://doi.org/10.1101/2022.06.14.496062; this version posted June 15, 2022. The copyright holder for this preprint (which was not certified by peer review) is the author/funder, who has granted bioRxiv a license to display the preprint in perpetuity. It is made available under aCC-BY 4.0 International license.

ordinal scale ranging from 3 to 1 (OS3 to 1) and a healthy control group. There was an equal contribution from PLWH and HIV-ve patients per group except for the control group. Three B cell phenotyping panels were used, focusing on homing (**A, B**); maturation (**C**) and regulatory (**D**) markers. Each panel included an anchor panel of CD19, IgD, IgM, CD27 and CD38. The key to the colouring of the different tSNE clusters is included alongside with a description of the phenotype. The phenotype is then depicted as a heatmap of the median fluorescence intensity (MFI) of each surface marker within that cluster, followed by a heatmap of the cluster frequency relative to ordinal scale (OS3 to 1); neutrophil lymphocyte ratio (NLR) cut-off of 3.0 to separate moderate and mild inflammation; SARS-CoV-2 viremia (S-CoV) and HIV status. (**B**) The frequency of each B cell phenotypic cluster identified by tSNE depicted as pie charts, separated based on disease severity (OS3 to 1) and controls.

Figure 3. Reduced germinal centre homing and class switching of memory B cells in HIV viraemic COVID-19 patients. (**A**) Gating strategy for total switched memory (SM; CD27+ IgD-) and homing to germinal centres (CD62L+ CXCR5+) and comparison of SM with respect to HIV status. (**B**) Germinal centre homing capacity relative to HIV status and longitudinal comparison. (**C**) The switched memory was further gated on IgM and IgD to identify IgM+ and class switched (IgM-IgD-) B cells. Both responses were compared with respect to HIV status. Statistical analyses were performed using the Kruskal-Wallis H test for multiple comparisons. *P* values are denoted by * ≤ 0.05; ** < 0.01; *** < 0.001 and **** < 0.0001.

Figure 4. Pronounced extrafollicular B cell activation in PLWH. (**A**) Naïve (CD27-IgD+) and double negative (DN; CD27-IgD-) B cell activation was measured as a CD21- CD95+ phenotype. The respective activated populations are thus DN2 and activated naïve. (**B**) Prevalence of the DN2 and activated naïve phenotypes with respect to HIV status. (**C**) The DN2 frequencies were tracked longitudinally and with respect to disease severity (Ordinal scale 1 to 3) and neutrophil lymphocyte ratio (NLR) respectively. (**D**) Spearman non-parametric correlation of the DN2 B cell response relative to the anti-RBD antibody titre. Statistical analyses were performed using the Kruskal-Wallis H test for multiple comparisons and Mann-Whitney for disease severity or NLR comparisons within groups. *P* values are denoted by * ≤ 0.05; ** < 0.01; *** < 0.001 and **** < 0.0001.

Figure 5. CD5+ PD-L1+ regulatory B cells contract during early response to infection. (**A**) Baseline (BL) and day 35 (D35+) example plots of a patient's CD5+ PD-L1+ regulatory B cell response. These cells were gated from the total naïve (CD27-) B cell population and their frequencies compared relative to HIV status. (**B**) This response was tracked longitudinally and relative to disease severity (ordinal scale 1 to 3) and controls denoted as "C". In (**C**) the corresponding CD4+ Tfh response was tracked longitudinally. Statistical analyses were performed using the Kruskal-Wallis H test for multiple comparisons and Mann-Whitney for disease severity. *P* values are denoted by * ≤ 0.05; ** < 0.01; *** < 0.001 and **** < 0.0001.

Figure 6. SARS-CoV-2 spike and receptor binding domain (RBD) specific B cell responses highlight an upregulated extrafollicular response in PLWH. The ancestral D614G viral spike (Spike-APC) and receptor binding domain (RBD-PE) proteins were used as baits to detect SARS-CoV-2 specific B cells with SA-APC and SA-PE used as controls (**A**). The bait specific B cells were then overlaid onto an IgM vs. IgD plot (**B**). The extent of IgM switched (MSM) and class switched memory (CSM) B cells were compared at both baseline (day 0) and day 84 post diagnosis. (**C**) Similarly, the level of CXCR3 expression was assessed. (**D**) The extent of double negative (DN) B cell activation (CD21- CD95+) was compared regarding HIV status at both time points. Statistical analyses were performed using Wilcoxon and Mann-Whitney tests. *P* values are denoted by * ≤ 0.05; ** < 0.01; *** < 0.001 and **** < 0.0001.

bioRxiv preprint doi: https://doi.org/10.1101/2022.06.14.496062; this version posted June 15, 2022. The copyright holder for this preprint (which was not certified by peer review) is the author/funder, who has granted bioRxiv a license to display the preprint in perpetuity. It is made available under aCC-BY 4.0 International license.

Extended Data Figure 1. Individual patient longitudinal ASC responses.

Extended Data Figure 2A. Heatmap overlays B cell compartment tSNE plots focusing on homing markers. A total of 80000 CD19+ B cells were used in an unbiased tSNE analysis of the B cell compartment with increasing disease severity ranked by ordinal scale 1 to 3 (OS1 to 3) and in healthy controls (Control). This means a total of 20000 CD19+ B cells were contributed by each group. The B cell homing marker expression is represented as a heat map with high (red) to low (blue) fluorescence intensity depicted.

Extended Data Figure 2B. Heatmap overlays B cell compartment tSNE plots focusing on maturation markers. A total of 80000 CD19+ B cells were used in an unbiased tSNE analysis of the B cell compartment with increasing disease severity ranked by ordinal scale 1 to 3 (OS1 to 3) and in healthy controls (Control). This means a total of 20000 CD19+ B cells were contributed by each group. The B cell maturation marker expression is represented as a heat map with high (red) to low (blue) fluorescence intensity depicted.

Extended Data Figure 2C. Heatmap overlays B cell compartment tSNE plots focusing on regulatory markers. A total of 80000 CD19+ B cells were used in an unbiased tSNE analysis of the B cell compartment with increasing disease severity ranked by ordinal scale 1 to 3 (OS1 to 3) and in healthy controls (Control). This means a total of 20000 CD19+ B cells were contributed by each group. The B cell regulatory marker expression is represented as a heat map with high (red) to low (blue) fluorescence intensity depicted.

Extended Data Figure 3. Individual patient longitudinal switched memory GC homing responses.

Extended Data Figure 4. Individual patient longitudinal DN2 and activated naïve B cell responses and detailed analysis of the activated naïve B cell response. Individual longitudinal DN2 (**A(i)**) and activated naïve (**A(ii)**) B cell responses. (**B**) The activated naïve B cell frequencies were tracked longitudinally and with respect to disease severity (Ordinal scale 1 to 3) and neutrophil lymphocyte ratio (NLR) respectively. (**C**) Spearman non-parametric correlation of the activated naïve B cell response relative to the anti-RBD antibody titre. Statistical analyses were performed using the Kruskal-Wallis H test for multiple comparisons and Mann-Whitney for disease severity or NLR comparisons within groups. *P* values are denoted by * ≤ 0.05; ** < 0.01; *** < 0.001 and **** < 0.0001.

Extended Data Figure 5. Individual patient longitudinal CD5+ PDL1+ B cell and Tfh responses.

Materials and methods

Ethical approval

The study protocol was approved by the University of KwaZulu-Natal Biomedical Research Ethics Committee (approval BREC/00001275/2020). Written informed consent was obtained for all enrolled participants.

Participant enrolment and clinical severity score

All study participants were over 18 years old and capable of giving informed consent; presented with a positive SARS-CoV-2 diagnosis and were recruited from two hospitals (King Edward VIII or Clairwood) in Durban, KwaZulu-Natal, South Africa, between 8 June and 25 September 2020. In total 126 participants were enrolled. Participants consented to blood and nasopharyngeal/oropharyngeal swab collection at recruitment and during weekly follow-up visits. All participant SARS-CoV-2 diagnoses were verified by an in-house RT-qPCR test which also served to quantify the SARS-CoV-2 viral load.

bioRxiv preprint doi: https://doi.org/10.1101/2022.06.14.496062; this version posted June 15, 2022. The copyright holder for this preprint (which was not certified by peer review) is the author/funder, who has granted bioRxiv a license to display the preprint in perpetuity. It is made available under aCC-BY 4.0 International license.

Two participants were excluded after their in-house RT-qPCR results remained negative and contradicted their initial diagnosis. All participants were ranked according to a clinical severity score of (1) asymptomatic, (2) symptomatic/mild without requiring supplemental oxygen and (3) moderate requiring supplemental oxygen. A total of 10 healthy controls were included in the study that tested SARS-CoV-2 negative by PCR and were seronegative by ELISA (described below).

Real Time-qPCR detection of SARS-CoV-2

The QIAmp Viral RNA Mini kit (cat. 52906, QIAGEN, Hilden, Germany) was used according to manufacturer's instructions to extract SARS-CoV-2 RNA from the combined nasopharyngeal and oropharyngeal swabs and 5 µl of the extracted RNA was used for RT-qPCR reactions. Three SARS-CoV-2 genes (ORF1ab, S and N) were amplified using the TaqPath COVID-19 Combo kit and TaqPath COVID-19 CE-IVD RT-PCR kit (ThermoFischer Scientific, MA, USA) using a QuantStudio 7 Flex Real-Time PCR system and analysed using the Design and Analysis software (ThermoFischer Scientific). Results were interpreted as positive if at least two of the three genes were amplified and regarded inconclusive if only one of the three genes were detected.

Clinical laboratory testing

A separate blood sample per participant was sent to an accredited diagnostic laboratory (Molecular Diagnostic Services, Durban, South Africa) for HIV testing by rapid test and quantification of HIV viral load using the RealTime HIV-1 viral load test on an Abbott machine. A full blood count, including CD4 and CD8 count, was performed by another accredited diagnostic laboratory (Ampath, Durban, South Africa).

Immune phenotyping of fresh PBMC by flow cytometry

Blood was collected in EDTA tubes and diluted 1 in 3 with PBS. Peripheral blood mononuclear cells (PBMC) were isolated by density gradient centrifugation through Histopaque 1077 (SIGMA) in SepMate separation tubes (STEMCELL Technologies, Vancouver Canada). For immune phenotyping 10^6 fresh PBMC were surface stained in a 25 µl antibody mix containing a LIVE/DEAD™ fixable near-IR-dead cell staining reagent (1:200 dilution, cat. L10119, Invitrogen, Carlsbad, CA, USA) with combinations of the listed antibodies (**Extended Data Table 1.**) from BD Biosciences (Franklin Lakes, NJ, USA); or from BioLegend (San Diego, CA, USA) or from Beckman Coulter (Brea, CA, USA). Cells were stained for 20 min in the dark at 4°C, followed by two 1 ml washes with cold PBS, then fixed in 2% paraformaldehyde and stored at 4°C until acquisition on a FACSAria Fusion III flow cytometer (BD). Flow cytometry data was analysed with FlowJo version 9.9.6 (Tree Star).

IgM and IgG ELISA detecting receptor binding domain specific antibodies

Patient plasma samples were tested for the presence of anti-SARS-CoV-2 reactive IgM or IgG antibodies as described previously (**Snyman *et al*., 2020**). ELISA plates were coated with 500 ng/ml of the D614G ancestral virus receptor binding domain (RBD) (GenBank: MN975262; provided by Dr Galit Alter, Ragon Institute, Cambridge, Massachusetts, USA) overnight at 4°C. Then blocked with 1% BSA-TBS at room temperature (RT) for 1 hour, followed by samples diluted at 1:100 in BSA-TBS + 0.05% Tween 20 for 1 hour at RT. Secondary anti-IgM or -IgG antibodies (Jackson ImmunoReasearch, West Grove, PA, USA) were added at 1:5000 diluted in BSA-TBS + 0.05% Tween 20 and incubated again for 1 hour at RT. Finally, plates were developed with 1-step Ultra TMB substrate (ThermoFischer Scientific) for 3 or 5 min respectively and signal development was stopped with the addition of 1 N H_2SO_4. Plates were washed with TBS + 0.05% Tween 20 between each incubation step. All signals were compared to anti-SARS-CoV-2 specific monoclonal IgG (clone CR3022) or IgM (clone hIgM2001). Pre-pandemic

bioRxiv preprint doi: https://doi.org/10.1101/2022.06.14.496062; this version posted June 15, 2022. The copyright holder for this preprint (which was not certified by peer review) is the author/funder, who has granted bioRxiv a license to display the preprint in perpetuity. It is made available under aCC-BY 4.0 International license.

plasma samples were used as negative controls to determine seroconversion cut-offs calculated as three times the standard deviation plus the mean.

Statistical analysis

All analyses were performed in Prism (v9; GraphPad Software Inc., San Diego, CA, USA). Nonparametric tests were used throughout, with Mann-Whitney and Wilcoxon tests used for unmatched and paired samples, respectively. Kruskal-Wallis H test was used for multiple comparisons. *P* values less than 0.05 were considered statistically significant and denoted by * ≤ 0.05; ** < 0.01; *** < 0.001 and **** < 0.0001.

References

Amu, S., Ruffin, N., Rethi, B., & Chiodi, F. (2013). Impairment of B-cell functions during HIV-1 infection. *AIDS, 27*(15), 2323-2334. doi:10.1097/QAD.0b013e328361a427

Bhaskaran, K., Rentsch, C. T., MacKenna, B., Schultze, A., Mehrkar, A., Bates, C. J., . . . Goldacre, B. (2021). HIV infection and COVID-19 death: a population-based cohort analysis of UK primary care data and linked national death registrations within the OpenSAFELY platform. *Lancet HIV, 8*(1), e24-e32. doi:10.1016/S2352-3018(20)30305-2

Catalan, D., Mansilla, M. A., Ferrier, A., Soto, L., Oleinika, K., Aguillon, J. C., & Aravena, O. (2021). Immunosuppressive Mechanisms of Regulatory B Cells. *Front Immunol, 12*, 611795. doi:10.3389/fimmu.2021.611795

Cele, S., Gazy, I., Jackson, L., Hwa, S. H., Tegally, H., Lustig, G., . . . Sigal, A. (2021). Escape of SARS-CoV-2 501Y.V2 from neutralization by convalescent plasma. *Nature, 593*(7857), 142-146. doi:10.1038/s41586-021-03471-w

Cele, S., Karim, F., Lustig, G., San, J. E., Hermanus, T., Tegally, H., . . . Sigal, A. (2022). SARS-CoV-2 prolonged infection during advanced HIV disease evolves extensive immune escape. *Cell Host Microbe, 30*(2), 154-162 e155. doi:10.1016/j.chom.2022.01.005

Chanda, D., Minchella, P. A., Kampamba, D., Itoh, M., Hines, J. Z., Fwoloshi, S., . . . Mulenga, L. B. (2021). COVID-19 Severity and COVID-19-Associated Deaths Among Hospitalized Patients with HIV Infection - Zambia, March-December 2020. *MMWR Morb Mortal Wkly Rep, 70*(22), 807-810. doi:10.15585/mmwr.mm7022a2

Chen, Y., Zuiani, A., Fischinger, S., Mullur, J., Atyeo, C., Travers, M., . . . Wesemann, D. R. (2020). Quick COVID-19 Healers Sustain Anti-SARS-CoV-2 Antibody Production. *Cell, 183*(6), 1496-1507 e1416. doi:10.1016/j.cell.2020.10.051

Ciccullo, A., Borghetti, A., Zileri Dal Verme, L., Tosoni, A., Lombardi, F., Garcovich, M., . . . Group, G. A. C. (2020). Neutrophil-to-lymphocyte ratio and clinical outcome in COVID-19: a report from the Italian front line. *Int J Antimicrob Agents, 56*(2), 106017. doi:10.1016/j.ijantimicag.2020.106017

Connolly, N. C., Riddler, S. A., & Rinaldo, C. R. (2005). Proinflammatory cytokines in HIV disease-a review and rationale for new therapeutic approaches. *AIDS Rev, 7*(3), 168-180. Retrieved from https://www.ncbi.nlm.nih.gov/pubmed/16302465

Cyster, J. G., & Allen, C. D. C. (2019). B Cell Responses: Cell Interaction Dynamics and Decisions. *Cell, 177*(3), 524-540. doi:10.1016/j.cell.2019.03.016

Dalgleish, A. G., Beverley, P. C., Clapham, P. R., Crawford, D. H., Greaves, M. F., & Weiss, R. A. (1984). The CD4 (T4) antigen is an essential component of the receptor for the AIDS retrovirus. *Nature, 312*(5996), 763-767. doi:10.1038/312763a0

Ehrhardt, G. R., Hsu, J. T., Gartland, L., Leu, C. M., Zhang, S., Davis, R. S., & Cooper, M. D. (2005). Expression of the immunoregulatory molecule FcRH4 defines a distinctive tissue-based population of memory B cells. *J Exp Med, 202*(6), 783-791. doi:10.1084/jem.20050879

Ferreira, C. B., Merino-Mansilla, A., Llano, A., Perez, I., Crespo, I., Llinas, L., . . . Sanchez-Merino, V. (2013). Evolution of broadly cross-reactive HIV-1-neutralizing activity: therapy-associated

bioRxiv preprint doi: https://doi.org/10.1101/2022.06.14.496062; this version posted June 15, 2022. The copyright holder for this preprint (which was not certified by peer review) is the author/funder, who has granted bioRxiv a license to display the preprint in perpetuity. It is made available under aCC-BY 4.0 International license.

539 decline, positive association with detectable viremia, and partial restoration of B-cell
540 subpopulations. *J Virol, 87*(22), 12227-12236. doi:10.1128/JVI.02155-13
541 Frater, J., Ewer, K. J., Ogbe, A., Pace, M., Adele, S., Adland, E., . . . Oxford, C. V. T. G. (2021). Safety and
542 immunogenicity of the ChAdOx1 nCoV-19 (AZD1222) vaccine against SARS-CoV-2 in HIV
543 infection: a single-arm substudy of a phase 2/3 clinical trial. *Lancet HIV, 8*(8), e474-e485.
544 doi:10.1016/S2352-3018(21)00103-X
545 Freudenhammer, M., Voll, R. E., Binder, S. C., Keller, B., & Warnatz, K. (2020). Naive- and Memory-like
546 CD21(low) B Cell Subsets Share Core Phenotypic and Signaling Characteristics in Systemic
547 Autoimmune Disorders. *J Immunol, 205*(8), 2016-2025. doi:10.4049/jimmunol.2000343
548 Fu, J., Kong, J., Wang, W., Wu, M., Yao, L., Wang, Z., . . . Yu, X. (2020). The clinical implication of dynamic
549 neutrophil to lymphocyte ratio and D-dimer in COVID-19: A retrospective study in Suzhou
550 China. *Thromb Res, 192*, 3-8. doi:10.1016/j.thromres.2020.05.006
551 Gaebler, C., Wang, Z., Lorenzi, J. C. C., Muecksch, F., Finkin, S., Tokuyama, M., . . . Nussenzweig, M. C.
552 (2021). Evolution of antibody immunity to SARS-CoV-2. *Nature, 591*(7851), 639-644.
553 doi:10.1038/s41586-021-03207-w
554 Glass, D. R., Tsai, A. G., Oliveria, J. P., Hartmann, F. J., Kimmey, S. C., Calderon, A. A., . . . Bendall, S. C.
555 (2020). An Integrated Multi-omic Single-Cell Atlas of Human B Cell Identity. *Immunity, 53*(1),
556 217-232 e215. doi:10.1016/j.immuni.2020.06.013
557 Goel, R. R., Apostolidis, S. A., Painter, M. M., Mathew, D., Pattekar, A., Kuthuru, O., . . . Wherry, E. J.
558 (2021). Distinct antibody and memory B cell responses in SARS-CoV-2 naive and recovered
559 individuals following mRNA vaccination. *Sci Immunol, 6*(58). doi:10.1126/sciimmunol.abi6950
560 Hassold, N., Brichler, S., Ouedraogo, E., Leclerc, D., Carroue, S., Gater, Y., . . . Delagreverie, H. (2022).
561 Impaired antibody response to COVID-19 vaccination in advanced HIV infection. *AIDS, 36*(4),
562 F1-F5. doi:10.1097/QAD.0000000000003166
563 Jenks, S. A., Cashman, K. S., Woodruff, M. C., Lee, F. E., & Sanz, I. (2019). Extrafollicular responses in
564 humans and SLE. *Immunol Rev, 288*(1), 136-148. doi:10.1111/imr.12741
565 Jenks, S. A., Cashman, K. S., Zumaquero, E., Marigorta, U. M., Patel, A. V., Wang, X., . . . Sanz, I. (2020).
566 Distinct Effector B Cells Induced by Unregulated Toll-like Receptor 7 Contribute to Pathogenic
567 Responses in Systemic Lupus Erythematosus. *Immunity, 52*(1), 203.
568 doi:10.1016/j.immuni.2019.12.005
569 Kaneko, N., Kuo, H. H., Boucau, J., Farmer, J. R., Allard-Chamard, H., Mahajan, V. S., . . . Massachusetts
570 Consortium on Pathogen Readiness Specimen Working, G. (2020). Loss of Bcl-6-Expressing T
571 Follicular Helper Cells and Germinal Centers in COVID-19. *Cell, 183*(1), 143-157 e113.
572 doi:10.1016/j.cell.2020.08.025
573 Karim, F., Gazy, I., Cele, S., Zungu, Y., Krause, R., Bernstein, M., . . . Sigal, A. (2021). HIV status alters
574 disease severity and immune cell responses in Beta variant SARS-CoV-2 infection wave. *Elife,*
575 *10*. doi:10.7554/eLife.67397
576 Kerneis, S., Launay, O., Turbelin, C., Batteux, F., Hanslik, T., & Boelle, P. Y. (2014). Long-term immune
577 responses to vaccination in HIV-infected patients: a systematic review and meta-analysis. *Clin*
578 *Infect Dis, 58*(8), 1130-1139. doi:10.1093/cid/cit937
579 Khan, A. R., Hams, E., Floudas, A., Sparwasser, T., Weaver, C. T., & Fallon, P. G. (2015). PD-L1hi B cells
580 are critical regulators of humoral immunity. *Nat Commun, 6*, 5997. doi:10.1038/ncomms6997
581 Kharsany, A. B. M., Cawood, C., Khanyile, D., Lewis, L., Grobler, A., Puren, A., . . . Abdool Karim, Q.
582 (2018). Community-based HIV prevalence in KwaZulu-Natal, South Africa: results of a cross-
583 sectional household survey. *Lancet HIV, 5*(8), e427-e437. doi:10.1016/S2352-3018(18)30104-
584 8
585 Knox, J. J., Buggert, M., Kardava, L., Seaton, K. E., Eller, M. A., Canaday, D. H., . . . Betts, M. R. (2017).
586 T-bet+ B cells are induced by human viral infections and dominate the HIV gp140 response.
587 *JCI Insight, 2*(8). doi:10.1172/jci.insight.92943

bioRxiv preprint doi: https://doi.org/10.1101/2022.06.14.496062; this version posted June 15, 2022. The copyright holder for this preprint (which was not certified by peer review) is the author/funder, who has granted bioRxiv a license to display the preprint in perpetuity. It is made available under aCC-BY 4.0 International license.

588 Lane, H. C., Masur, H., Edgar, L. C., Whalen, G., Rook, A. H., & Fauci, A. S. (1983). Abnormalities of B-
589 cell activation and immunoregulation in patients with the acquired immunodeficiency
590 syndrome. *N Engl J Med, 309*(8), 453-458. doi:10.1056/NEJM198308253090803
591 Le Gallo, M., Poissonnier, A., Blanco, P., & Legembre, P. (2017). CD95/Fas, Non-Apoptotic Signaling
592 Pathways, and Kinases. *Front Immunol, 8*, 1216. doi:10.3389/fimmu.2017.01216
593 McCormick, K. D., Jacobs, J. L., & Mellors, J. W. (2021). The emerging plasticity of SARS-CoV-2. *Science,*
594 *371*(6536), 1306-1308. doi:10.1126/science.abg4493
595 Moir, S., & Fauci, A. S. (2014). B-cell exhaustion in HIV infection: the role of immune activation. *Curr*
596 *Opin HIV AIDS, 9*(5), 472-477. doi:10.1097/COH.0000000000000092
597 Muecksch, F., Weisblum, Y., Barnes, C. O., Schmidt, F., Schaefer-Babajew, D., Wang, Z., . . . Bieniasz, P.
598 D. (2021). Affinity maturation of SARS-CoV-2 neutralizing antibodies confers potency, breadth,
599 and resilience to viral escape mutations. *Immunity, 54*(8), 1853-1868 e1857.
600 doi:10.1016/j.immuni.2021.07.008
601 Okoye, A. A., & Picker, L. J. (2013). CD4(+) T-cell depletion in HIV infection: mechanisms of
602 immunological failure. *Immunol Rev, 254*(1), 54-64. doi:10.1111/imr.12066
603 Oleinika, K., Rosser, E. C., Matei, D. E., Nistala, K., Bosma, A., Drozdov, I., & Mauri, C. (2018). CD1d-
604 dependent immune suppression mediated by regulatory B cells through modulations of iNKT
605 cells. *Nat Commun, 9*(1), 684. doi:10.1038/s41467-018-02911-y
606 Onodera, T., Takahashi, Y., Yokoi, Y., Ato, M., Kodama, Y., Hachimura, S., . . . Kobayashi, K. (2012).
607 Memory B cells in the lung participate in protective humoral immune responses to pulmonary
608 influenza virus reinfection. *Proc Natl Acad Sci U S A, 109*(7), 2485-2490.
609 doi:10.1073/pnas.1115369109
610 Pallikkuth, S., Parmigiani, A., Silva, S. Y., George, V. K., Fischl, M., Pahwa, R., & Pahwa, S. (2012).
611 Impaired peripheral blood T-follicular helper cell function in HIV-infected nonresponders to
612 the 2009 H1N1/09 vaccine. *Blood, 120*(5), 985-993. doi:10.1182/blood-2011-12-396648
613 Palmer, V. L., Nganga, V. K., Rothermund, M. E., Perry, G. A., & Swanson, P. C. (2015). Cd1d regulates
614 B cell development but not B cell accumulation and IL10 production in mice with pathologic
615 CD5(+) B cell expansion. *BMC Immunol, 16*, 66. doi:10.1186/s12865-015-0130-z
616 Perreau, M., Savoye, A. L., De Crignis, E., Corpataux, J. M., Cubas, R., Haddad, E. K., . . . Pantaleo, G.
617 (2013). Follicular helper T cells serve as the major CD4 T cell compartment for HIV-1 infection,
618 replication, and production. *J Exp Med, 210*(1), 143-156. doi:10.1084/jem.20121932
619 Reimer, D., Lee, A. Y., Bannan, J., Fromm, P., Kara, E. E., Comerford, I., . . . Korner, H. (2017). Early CCR6
620 expression on B cells modulates germinal centre kinetics and efficient antibody responses.
621 *Immunol Cell Biol, 95*(1), 33-41. doi:10.1038/icb.2016.68
622 Roff, S. R., Noon-Song, E. N., & Yamamoto, J. K. (2014). The Significance of Interferon-gamma in HIV-1
623 Pathogenesis, Therapy, and Prophylaxis. *Front Immunol, 4*, 498.
624 doi:10.3389/fimmu.2013.00498
625 Serre, K., Cunningham, A. F., Coughlan, R. E., Lino, A. C., Rot, A., Hub, E., . . . Mohr, E. (2012). CD8 T
626 cells induce T-bet-dependent migration toward CXCR3 ligands by differentiated B cells
627 produced during responses to alum-protein vaccines. *Blood, 120*(23), 4552-4559.
628 doi:10.1182/blood-2012-03-417733
629 Sette, A., & Crotty, S. (2021). Adaptive immunity to SARS-CoV-2 and COVID-19. *Cell, 184*(4), 861-880.
630 doi:10.1016/j.cell.2021.01.007
631 Shinde, V., Bhikha, S., Hoosain, Z., Archary, M., Bhorat, Q., Fairlie, L., . . . nCo, V. S. G. (2021). Efficacy
632 of NVX-CoV2373 Covid-19 Vaccine against the B.1.351 Variant. *N Engl J Med, 384*(20), 1899-
633 1909. doi:10.1056/NEJMoa2103055
634 Snyman, J., Hwa, S. H., Krause, R., Muema, D., Reddy, T., Ganga, Y., . . . Team, C.-K. (2021). Similar
635 antibody responses against SARS-CoV-2 in HIV uninfected and infected individuals on
636 antiretroviral therapy during the first South African infection wave. *Clin Infect Dis*.
637 doi:10.1093/cid/ciab758

bioRxiv preprint doi: https://doi.org/10.1101/2022.06.14.496062; this version posted June 15, 2022. The copyright holder for this preprint (which was not certified by peer review) is the author/funder, who has granted bioRxiv a license to display the preprint in perpetuity. It is made available under aCC-BY 4.0 International license.

638 Sun, X., Zhang, T., Li, M., Yin, L., & Xue, J. (2019). Immunosuppressive B cells expressing PD-1/PD-L1 in
639 solid tumors: A mini review. *QJM*. doi:10.1093/qjmed/hcz162
640 Sutton, H. J., Aye, R., Idris, A. H., Vistein, R., Nduati, E., Kai, O., . . . Cockburn, I. A. (2021). Atypical B
641 cells are part of an alternative lineage of B cells that participates in responses to vaccination
642 and infection in humans. *Cell Rep, 34*(6), 108684. doi:10.1016/j.celrep.2020.108684
643 Tada, T., Zhou, H., Samanovic, M. I., Dcosta, B. M., Cornelius, A., Mulligan, M. J., & Landau, N. R. (2021).
644 Comparison of Neutralizing Antibody Titers Elicited by mRNA and Adenoviral Vector Vaccine
645 against SARS-CoV-2 Variants. *bioRxiv*. doi:10.1101/2021.07.19.452771
646 Tegally, H., Wilkinson, E., Giovanetti, M., Iranzadeh, A., Fonseca, V., Giandhari, J., . . . de Oliveira, T.
647 (2021). Detection of a SARS-CoV-2 variant of concern in South Africa. *Nature, 592*(7854), 438-
648 443. doi:10.1038/s41586-021-03402-9
649 van der Maaten L., H. G. (2008). Visualizing Data using t-SNE. *Journal of Machine Learning Research,*
650 *9*, 2579-2605.
651 Van Gassen, S., Callebaut, B., Van Helden, M. J., Lambrecht, B. N., Demeester, P., Dhaene, T., & Saeys,
652 Y. (2015). FlowSOM: Using self-organizing maps for visualization and interpretation of
653 cytometry data. *Cytometry A, 87*(7), 636-645. doi:10.1002/cyto.a.22625
654 Wang, Z., Schmidt, F., Weisblum, Y., Muecksch, F., Barnes, C. O., Finkin, S., . . . Nussenzweig, M. C.
655 (2021). mRNA vaccine-elicited antibodies to SARS-CoV-2 and circulating variants. *Nature,*
656 *592*(7855), 616-622. doi:10.1038/s41586-021-03324-6
657 Weill, J. C., & Reynaud, C. A. (2020). IgM memory B cells: specific effectors of innate-like and adaptive
658 responses. *Curr Opin Immunol, 63*, 1-6. doi:10.1016/j.coi.2019.09.003
659 Weisel, N. M., Weisel, F. J., Farber, D. L., Borghesi, L. A., Shen, Y., Ma, W., . . . Shlomchik, M. J. (2020).
660 Comprehensive analyses of B-cell compartments across the human body reveal novel subsets
661 and a gut-resident memory phenotype. *Blood, 136*(24), 2774-2785.
662 doi:10.1182/blood.2019002782
663 Westendorp, M. O., Frank, R., Ochsenbauer, C., Stricker, K., Dhein, J., Walczak, H., . . . Krammer, P. H.
664 (1995). Sensitization of T cells to CD95-mediated apoptosis by HIV-1 Tat and gp120. *Nature,*
665 *375*(6531), 497-500. doi:10.1038/375497a0
666 Western Cape Department of Health in collaboration with the National Institute for Communicable
667 Diseases, S. A. (2021). Risk Factors for Coronavirus Disease 2019 (COVID-19) Death in a
668 Population Cohort Study from the Western Cape Province, South Africa. *Clin Infect Dis, 73*(7),
669 e2005-e2015. doi:10.1093/cid/ciaa1198
670 Wibmer, C. K., Ayres, F., Hermanus, T., Madzivhandila, M., Kgagudi, P., Oosthuysen, B., . . . Moore, P.
671 L. (2021). SARS-CoV-2 501Y.V2 escapes neutralization by South African COVID-19 donor
672 plasma. *Nat Med, 27*(4), 622-625. doi:10.1038/s41591-021-01285-x
673 Wiede, F., Fromm, P. D., Comerford, I., Kara, E., Bannan, J., Schuh, W., . . . Korner, H. (2013). CCR6 is
674 transiently upregulated on B cells after activation and modulates the germinal center reaction
675 in the mouse. *Immunol Cell Biol, 91*(5), 335-339. doi:10.1038/icb.2013.14
676 Williamson, E. J., Walker, A. J., Bhaskaran, K., Bacon, S., Bates, C., Morton, C. E., . . . Goldacre, B. (2020).
677 Factors associated with COVID-19-related death using OpenSAFELY. *Nature, 584*(7821), 430-
678 436. doi:10.1038/s41586-020-2521-4
679 Woodruff, M. C., Ramonell, R. P., Nguyen, D. C., Cashman, K. S., Saini, A. S., Haddad, N. S., . . . Sanz, I.
680 (2020). Extrafollicular B cell responses correlate with neutralizing antibodies and morbidity in
681 COVID-19. *Nat Immunol, 21*(12), 1506-1516. doi:10.1038/s41590-020-00814-z
682 Yanaba, K., Bouaziz, J. D., Haas, K. M., Poe, J. C., Fujimoto, M., & Tedder, T. F. (2008). A regulatory B
683 cell subset with a unique CD1dhiCD5+ phenotype controls T cell-dependent inflammatory
684 responses. *Immunity, 28*(5), 639-650. doi:10.1016/j.immuni.2008.03.017
685 Zohar, T., Loos, C., Fischinger, S., Atyeo, C., Wang, C., Slein, M. D., . . . Alter, G. (2020). Compromised
686 Humoral Functional Evolution Tracks with SARS-CoV-2 Mortality. *Cell, 183*(6), 1508-1519
687 e1512. doi:10.1016/j.cell.2020.10.052

688

bioRxiv preprint doi: https://doi.org/10.1101/2022.06.14.496062; this version posted June 15, 2022. The copyright holder for this preprint (which was not certified by peer review) is the author/funder, who has granted bioRxiv a license to display the preprint in perpetuity. It is made available under aCC-BY 4.0 International license.

689

690

691

692

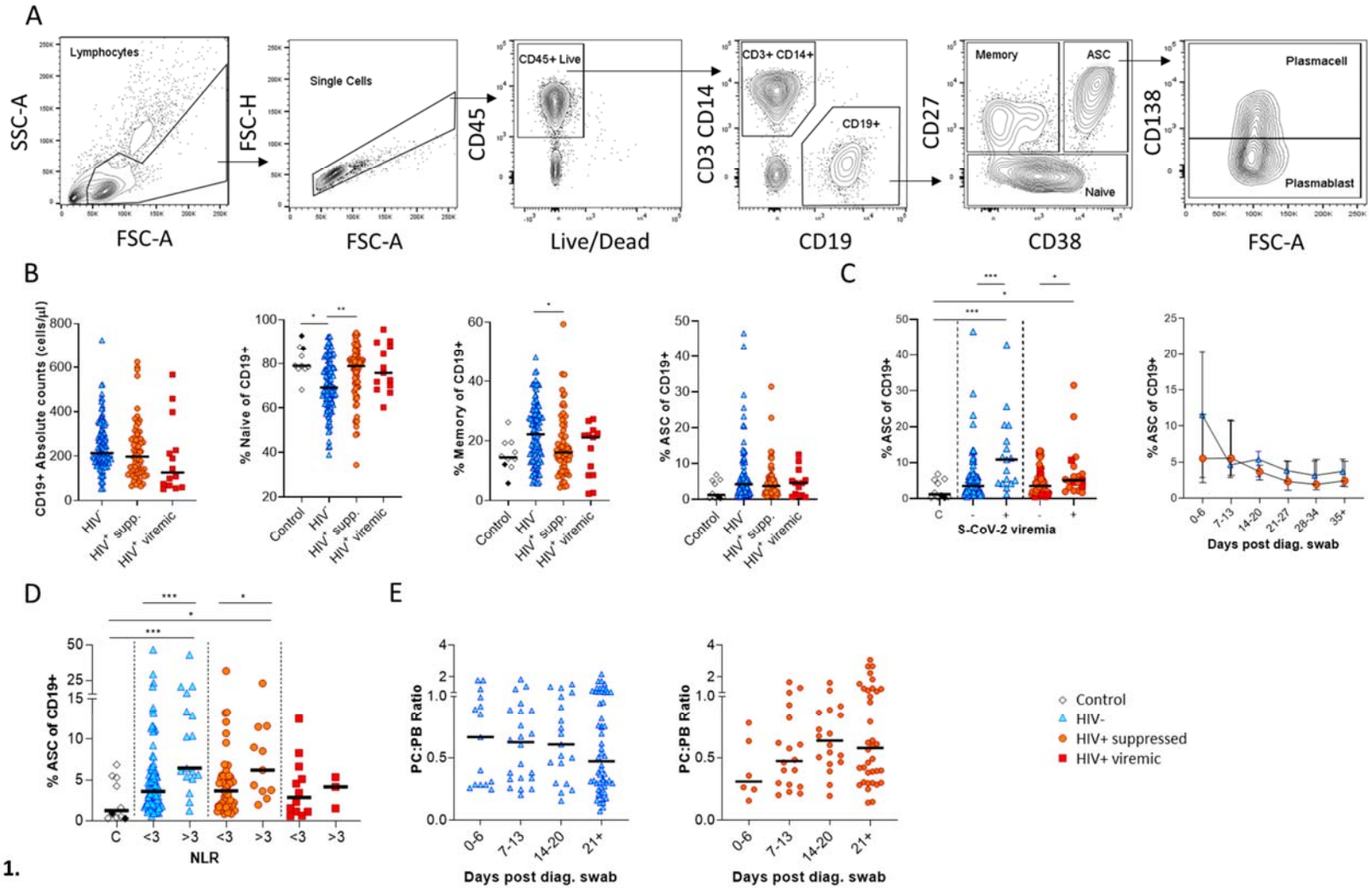
A
Lymphocytes
SSC-A
FSC-A
Single Cells
FSC-H
FSC-A
CD45+ Live
CD45
Live/Dead
CD3+ CD14+
CD3 CD14
CD19+
CD19
Memory
ASC
Naive
CD27
CD38
Plasmacell
Plasmablast
CD138
FSC-A
B
CD19+ Absolute counts (cells/µl)
% Naive of CD19+
% Memory of CD19+
% ASC of CD19+
Control
HIV-
HIV+ supp.
HIV+ viremic
C
% ASC of CD19+
S-CoV-2 viremia
% ASC of CD19+
Days post diag. swab
D
% ASC of CD19+
NLR
E
PC:PB Ratio
Days post diag. swab
PC:PB Ratio
Days post diag. swab
Control
HIV-
HIV+ suppressed
HIV+ viremic

Figure 1.

bioRxiv preprint doi: https://doi.org/10.1101/2022.06.14.496062; this version posted June 15, 2022. The copyright holder for this preprint (which was not certified by peer review) is the author/funder, who has granted bioRxiv a license to display the preprint in perpetuity. It is made available under aCC-BY 4.0 International license.

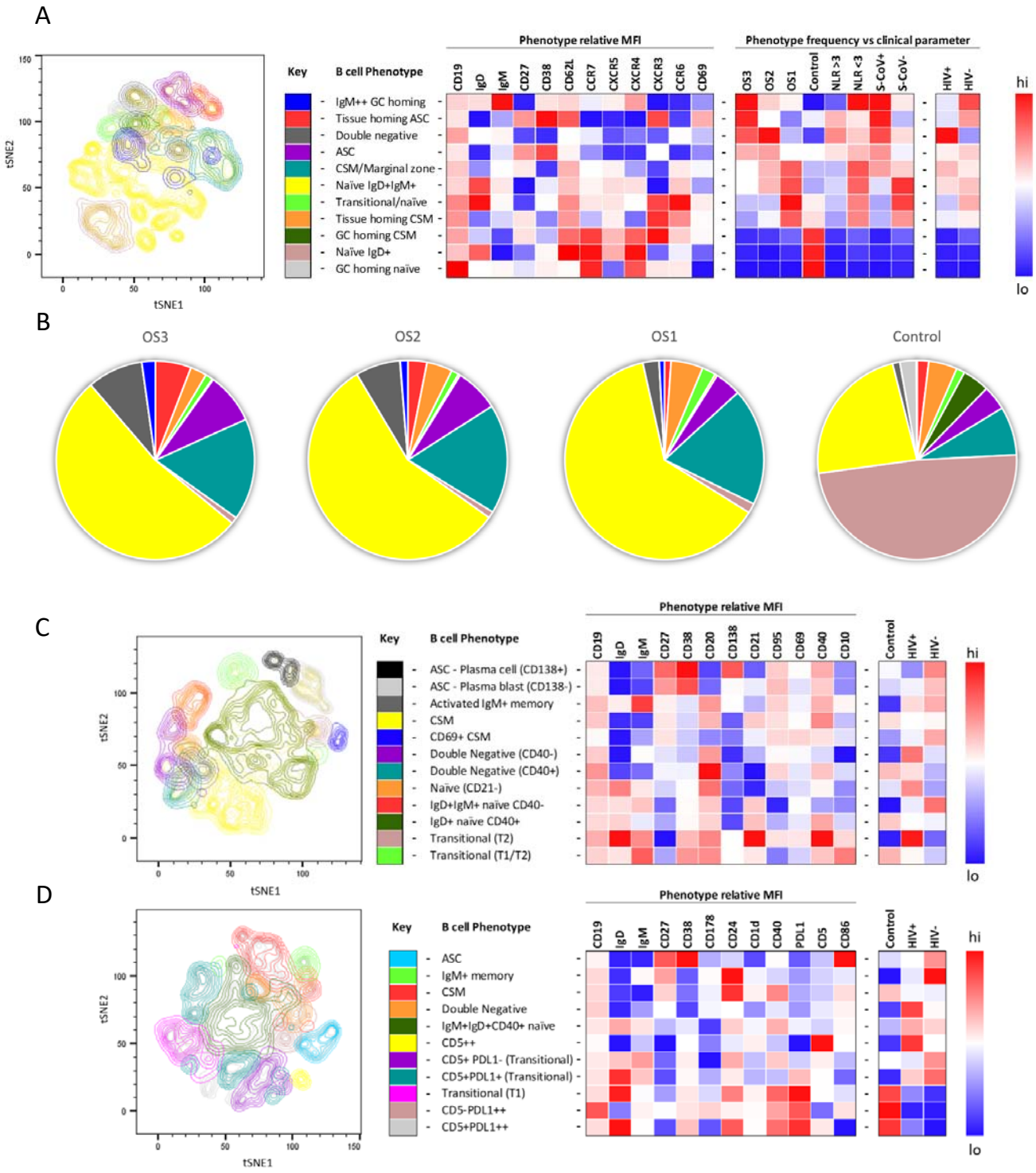

Figure 2.

bioRxiv preprint doi: https://doi.org/10.1101/2022.06.14.496062; this version posted June 15, 2022. The copyright holder for this preprint (which was not certified by peer review) is the author/funder, who has granted bioRxiv a license to display the preprint in perpetuity. It is made available under aCC-BY 4.0 International license.

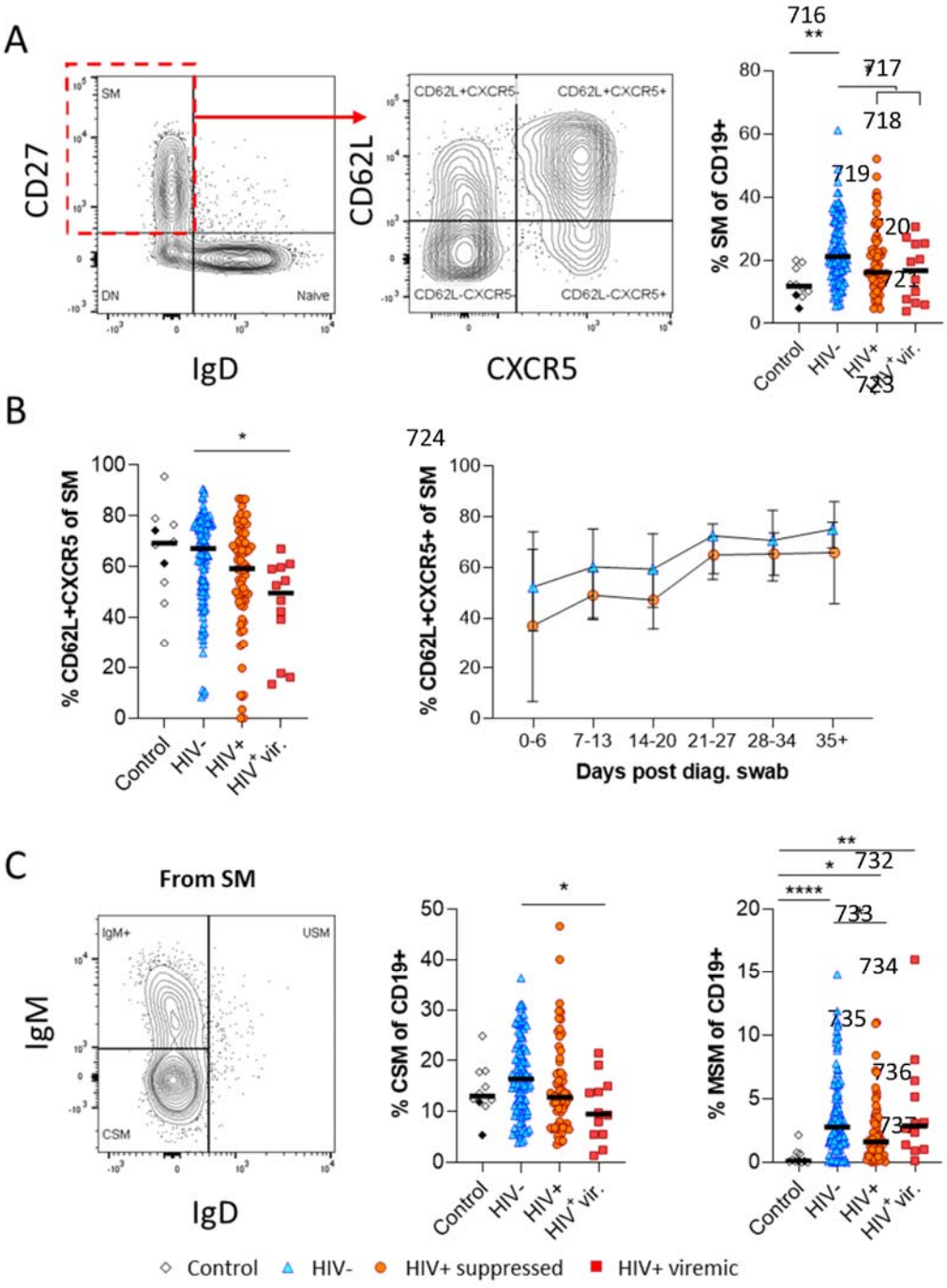

742 **Figure 3**

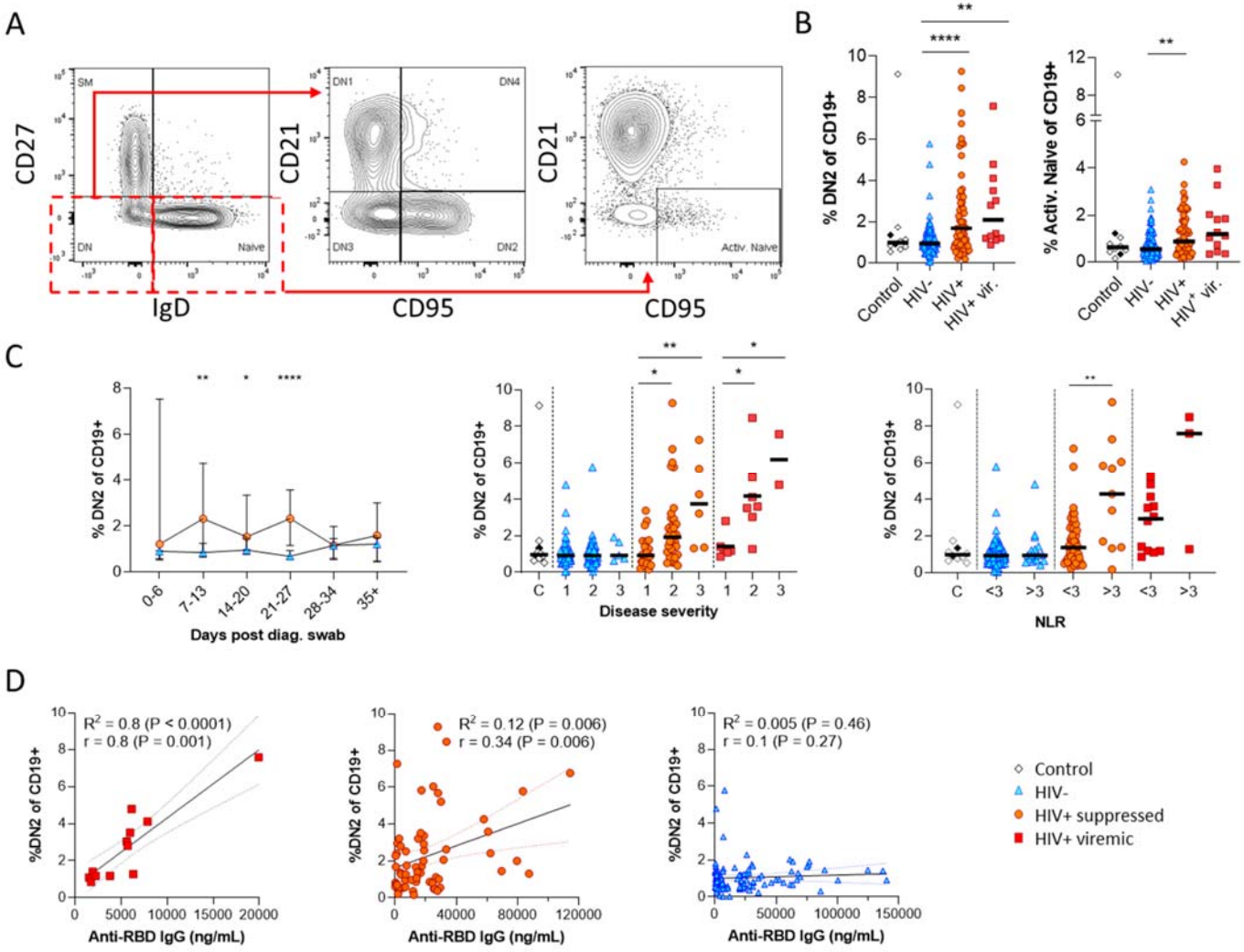
A
CD27
IgD
SM
DN
Naive
CD21
CD95
DN1
DN4
DN3
DN2
CD21
CD95
Activ. Naive
B
% DN2 of CD19+
Control
HIV-
HIV+
HIV+ vir.
% Activ. Naive of CD19+
C
% DN2 of CD19+
Days post diag. swab
0-6
7-13
14-20
21-27
28-34
35+
Disease severity
NLR
D
%DN2 of CD19+
R² = 0.8 (P < 0.0001)
r = 0.8 (P = 0.001)
Anti-RBD IgG (ng/mL)
R² = 0.12 (P = 0.006)
r = 0.34 (P = 0.006)
R² = 0.005 (P = 0.46)
r = 0.1 (P = 0.27)
Control
HIV-
HIV+ suppressed
HIV+ viremic

Figure 4.

bioRxiv preprint doi: https://doi.org/10.1101/2022.06.14.496062; this version posted June 15, 2022. The copyright holder for this preprint (which was not certified by peer review) is the author/funder, who has granted bioRxiv a license to display the preprint in perpetuity. It is made available under aCC-BY 4.0 International license.

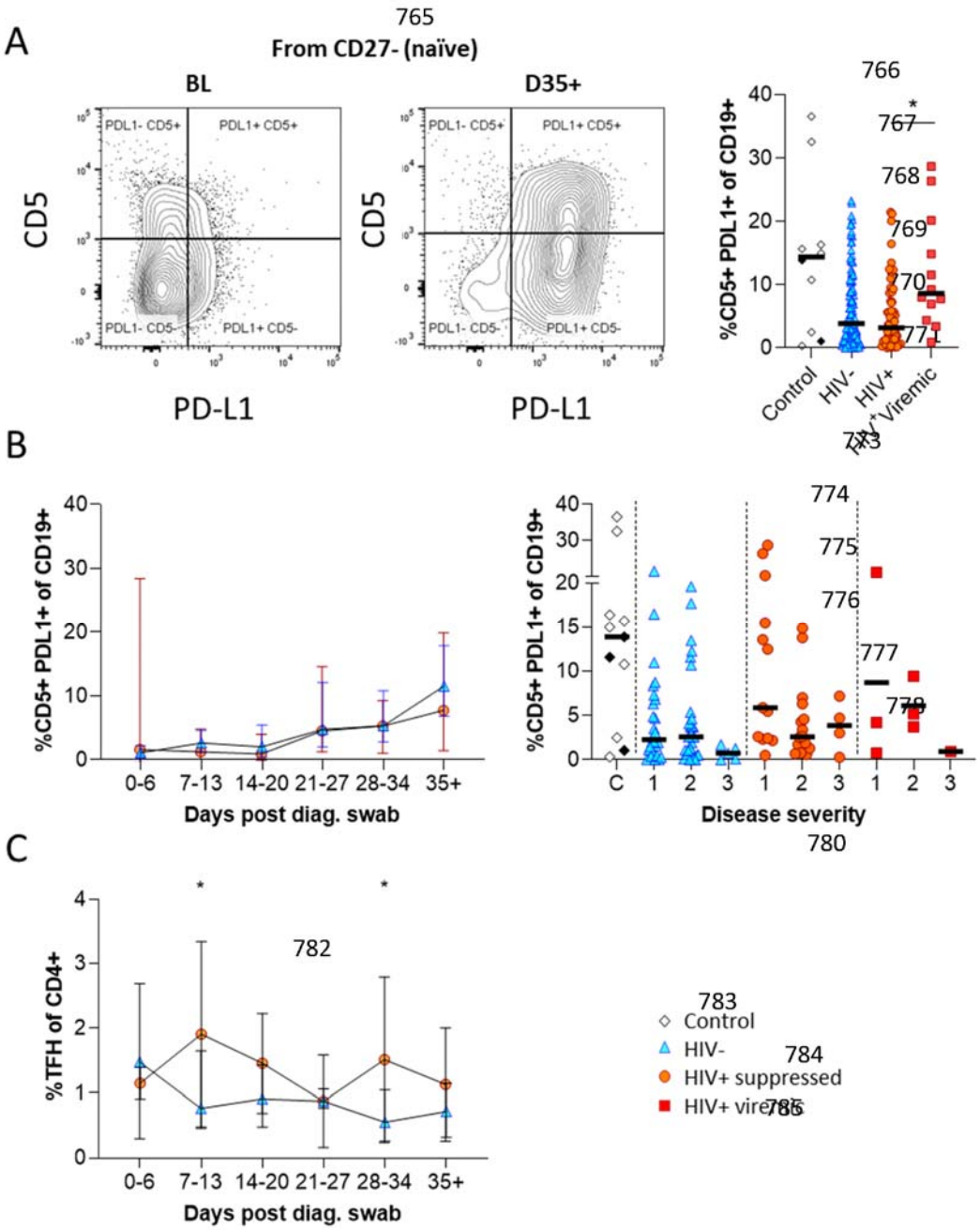

Figure 5.

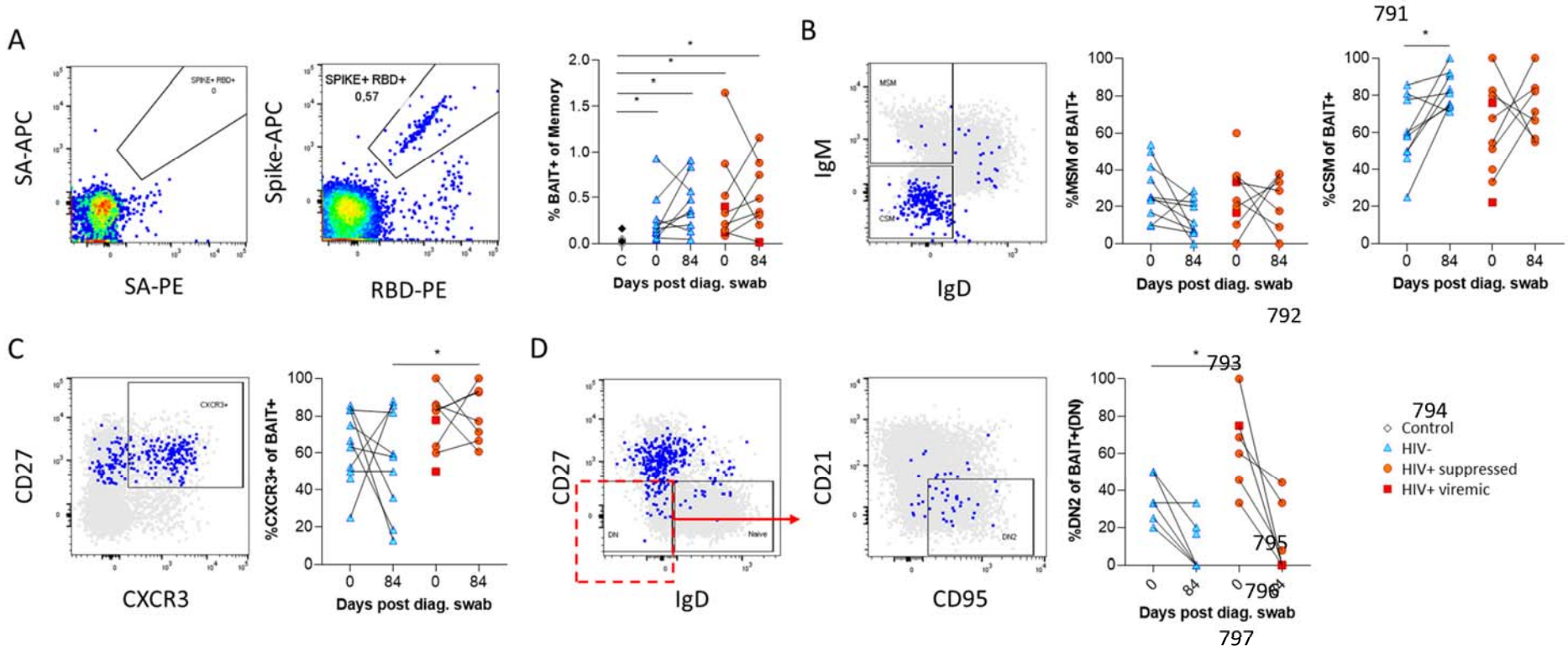
A
SA-APC
SA-PE
SPIKE+ RBD+
0
Spike-APC
RBD-PE
SPIKE+ RBD+
0,57
% BAIT+ of Memory
C
0
84
0
84
Days post diag. swab
B
IgM
IgD
MSM
CSM
%MSM of BAIT+
%CSM of BAIT+
Days post diag. swab
C
CD27
CXCR3
CXCR3+
%CXCR3+ of BAIT+
Days post diag. swab
D
CD27
IgD
DN
Naive
CD21
CD95
DN2
%DN2 of BAIT+(DN)
Days post diag. swab
Control
HIV-
HIV+ suppressed
HIV+ viremic

Figure 6.

bioRxiv preprint doi: https://doi.org/10.1101/2022.06.14.496062; this version posted June 15, 2022. The copyright holder for this preprint (which was not certified by peer review) is the author/funder, who has granted bioRxiv a license to display the preprint in perpetuity. It is made available under aCC-BY 4.0 International license.

Extended Data Table 1. Flow Cytometry B cell phenotyping antibody panels

Panel	Marker	Label	clone	cat no	Supplier
Core	L/D	APC-Cy7		L10119	Invitrogen
	CD45	APC	HI30	304012	BioLegend
	CD3	Bv711	OKT3	317328	BioLegend
	CD14	Bv711	M5E2	301838	BioLegend
	CD19	Bv605	HIB19	302244	BioLegend
	CD27	Bv510	O323	302836	BioLegend
	CD38	PECy7	HIT2	303516	BioLegend
	IgM	PerCP/Cy5.5	MHM-88	314512	BioLegend
	IgD	AF700	IA6-2	348230	BioLegend
Homing	CD27	Bv510	O323	302836	BioLegend
	CCR6 (CD196)	Bv421	GO34E3	353439	BioLegend
	CXCR5	AF488 (FITC)	RF8B2	558112	BD Pharmingen
	CXCR4 (CD184)	Bv785™	12G5	306530	BioLegend
	CD62L	PE-Cy5	DREG-56	555545	BD Pharmingen
	CXCR3 (CD183)	PE-CF594	IC6/CXCR3	562451	BD Horizon
	CD69	BUV395	FN50	564364	BD Horizon
	CCR7	PE	150503	FAB197P	R&D Biosystems
Maturation	CD27	Bv510	O323	302836	BioLegend
	CD138 (Syndecan-1)	Bv785™	MI15	356538	BioLegend
	CXCR5	AF488 (FITC)	RF8B2	558112	BD Pharmingen
	CD11c	PE	S-HCL-3	371504	BioLegend
	CD95 (Fas)	Bv650™	DX2	305642	BioLegend
	CD20	PE/Dazzle™ 594	2H7	302348	BioLegend
	CD69	BUV395	FN50	564364	BD Horizon
	CD10	PE-Cy5	HI10a (RUO)	555376	BD Pharmingen
	CD21	Bv421	B-ly4	562966	BD Horizon
	CD40	BUV496	5C3	741159	BD OptiBuild
Regulatory	CD27	PE-Cy5	1A4CD27	6607107	Beckman Coulter
	CD40	BUV496	5C3	741159	BD OptiBuild
	PD-L1 (CD274)	PE	29E.2A3	329706	BioLegend
	CD24	FITC	ML5	311104	BioLegend
	CD178 (Fas-L)	Bv421™	NOK-1	306412	BioLegend
	CD1d	Bv510™	51.1	350314	BioLegend
	CD5	PE/Dazzle™ 594	L17F12	364012	BioLegend
	CD86	Bv650™	IT2.2	305428	BioLegend

bioRxiv preprint doi: https://doi.org/10.1101/2022.06.14.496062; this version posted June 15, 2022. The copyright holder for this preprint (which was not certified by peer review) is the author/funder, who has granted bioRxiv a license to display the preprint in perpetuity. It is made available under aCC-BY 4.0 International license.

808 **Extended Data Table 2. Flow Cytometry B cell BAIT antibody panel**

Marker	Label	clone	cat no	Supplier
L/D	APC-Cy7		L10119	Invitrogen
CD45	Hv500	HI30	560777	BD Horizon
CD3	Bv711	OKT3	317328	BioLegend
CD14	Bv711	M5E2	301838	BioLegend
CD19	Bv605	HIB19	302244	BioLegend
CD27	PE-Cy5	1A4CD27	6607107	Beckman Coulter
CD38	PECy7	HIT2	303516	BioLegend
IgM	PerCP/Cy5.5	MHM-88	314512	BioLegend
IgD	AF700	IA6-2	348230	BioLegend
CXCR3	PE-CF594	IC6/CXCR3	562451	BD Horizon
CD21	Bv421	B-ly4	562966	BD Horizon
BAIT	SA-APC		405207	BioLegend
BIAT	SA-PE		405204	BioLegend

809

810

811

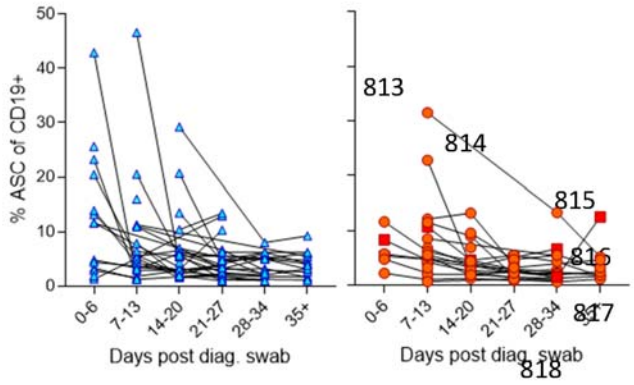

819

820 **Extended data Figure 1.**

821

822

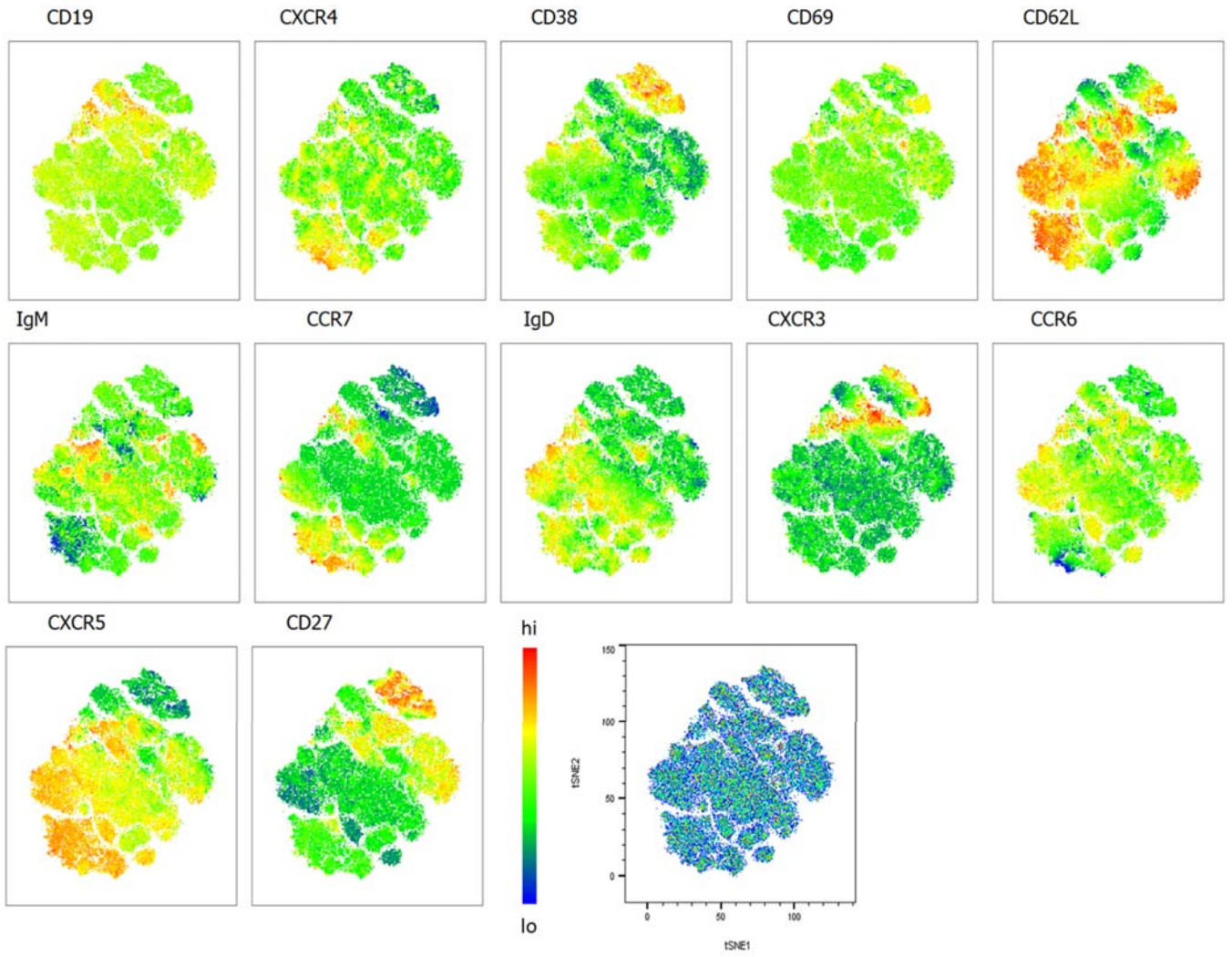

Extended Data Figure 2A.

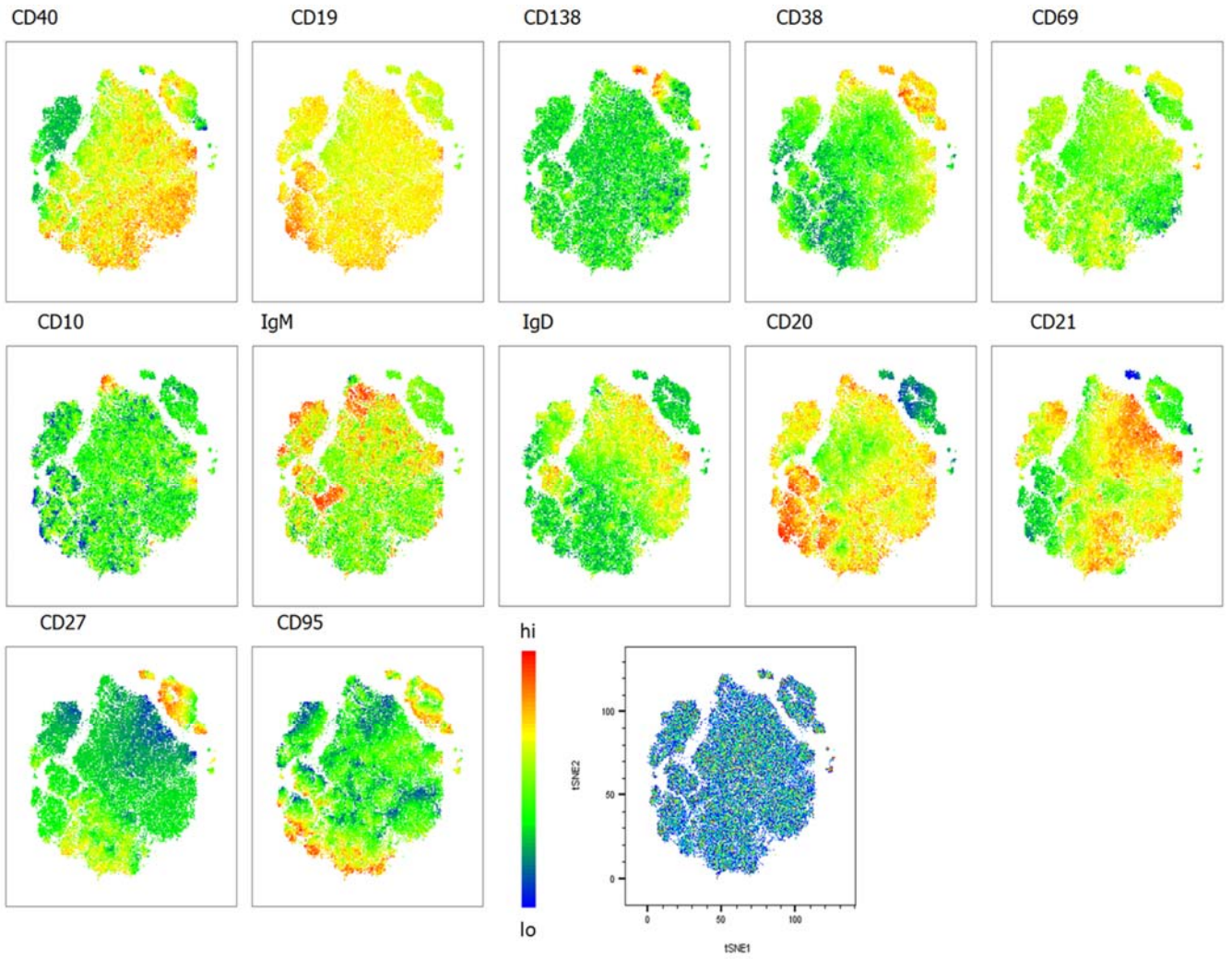

Extended Data Figure 2B.

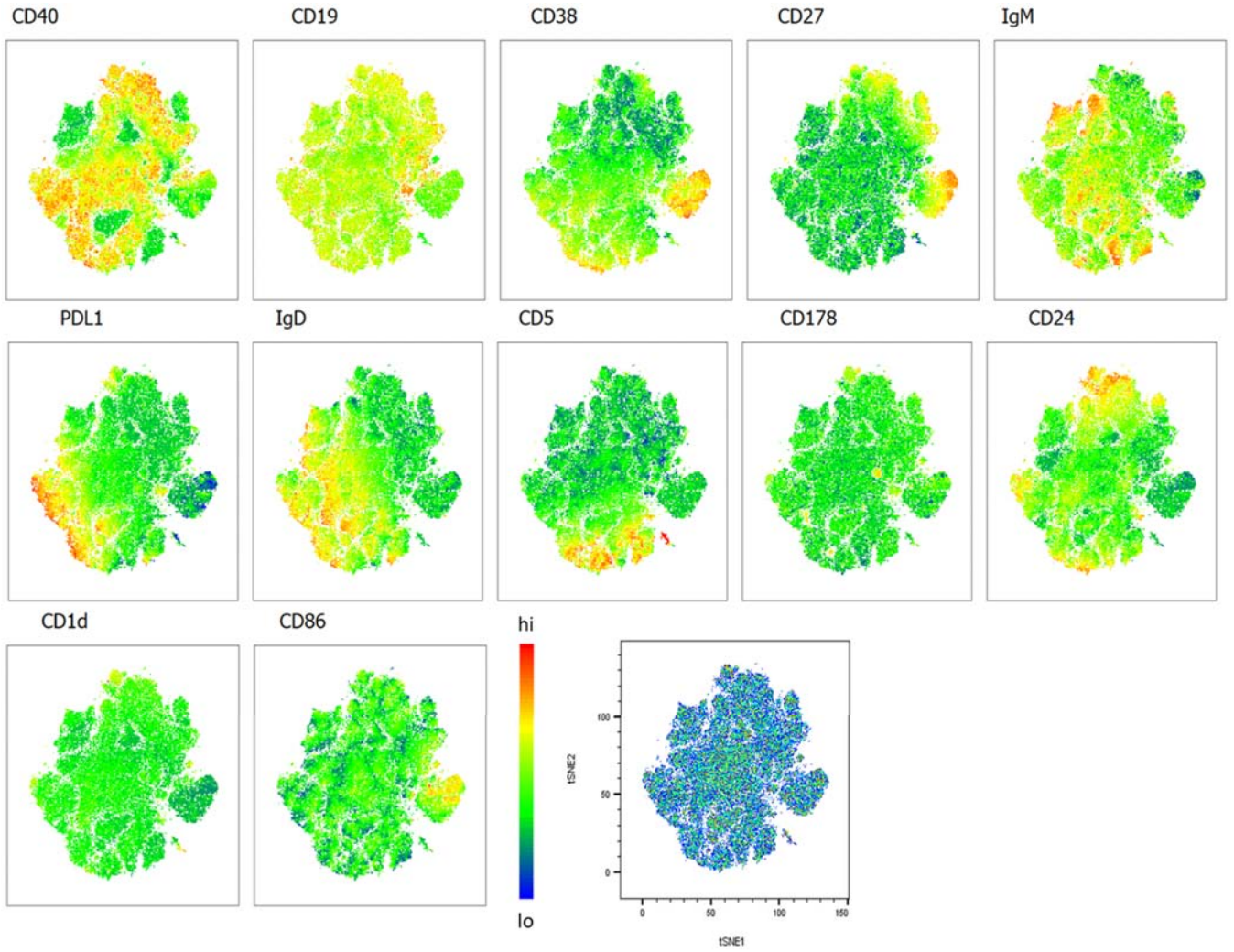

Extended Data Figure 2C

bioRxiv preprint doi: https://doi.org/10.1101/2022.06.14.496062; this version posted June 15, 2022. The copyright holder for this preprint (which was not certified by peer review) is the author/funder, who has granted bioRxiv a license to display the preprint in perpetuity. It is made available under aCC-BY 4.0 International license.

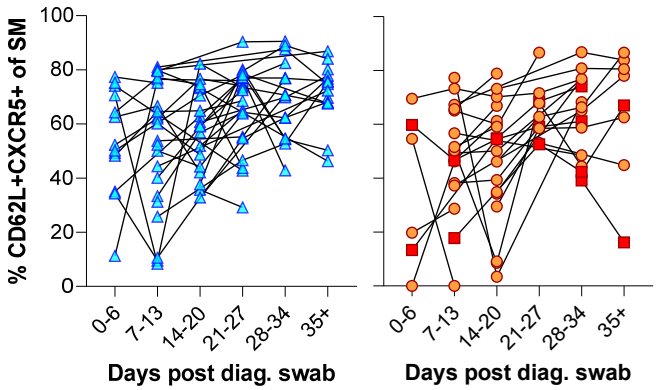

Extended Data Figure 3.

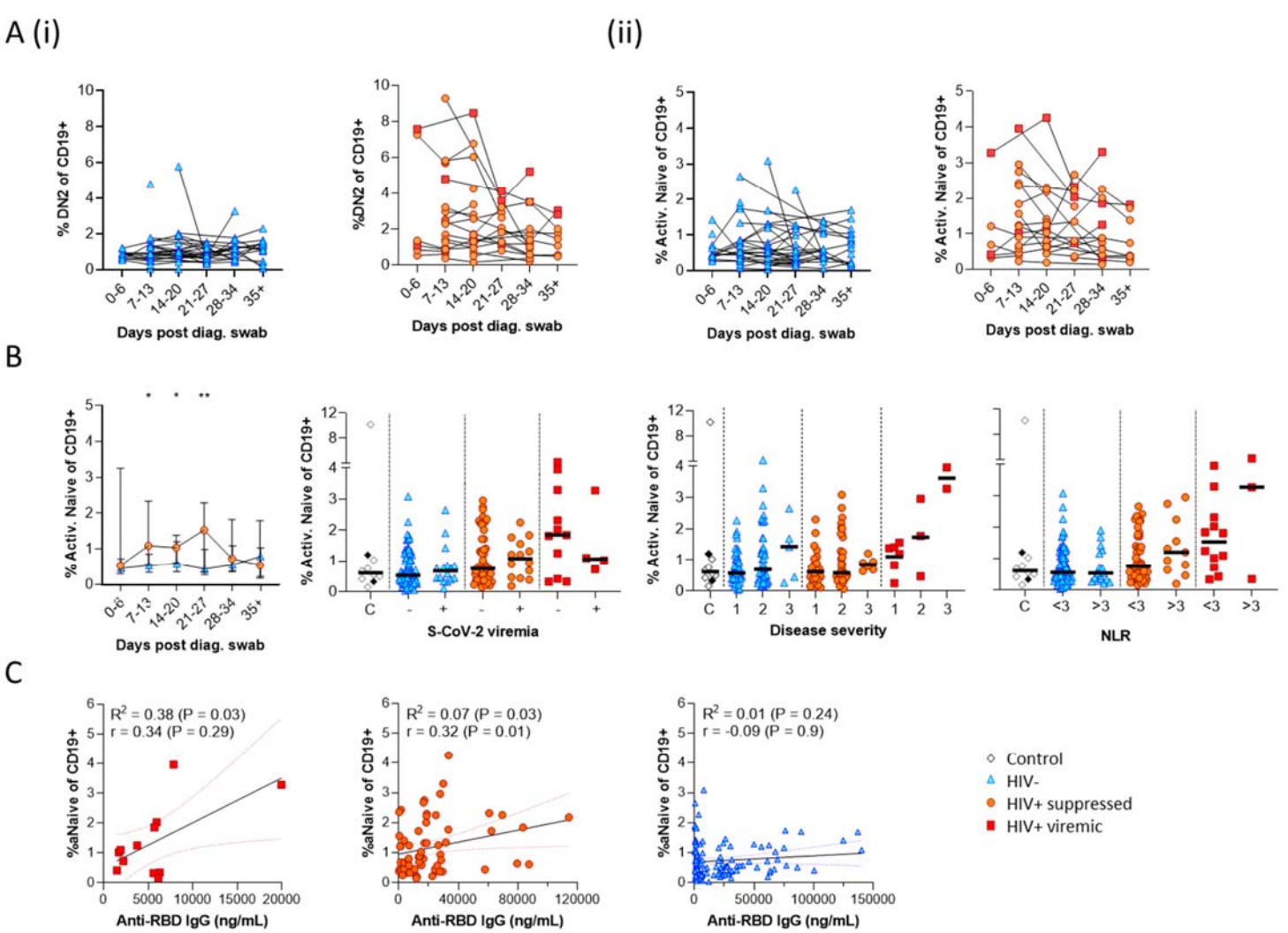

Extended Data Figure 4.

bioRxiv preprint doi: https://doi.org/10.1101/2022.06.14.496062; this version posted June 15, 2022. The copyright holder for this preprint (which was not certified by peer review) is the author/funder, who has granted bioRxiv a license to display the preprint in perpetuity. It is made available under aCC-BY 4.0 International license.

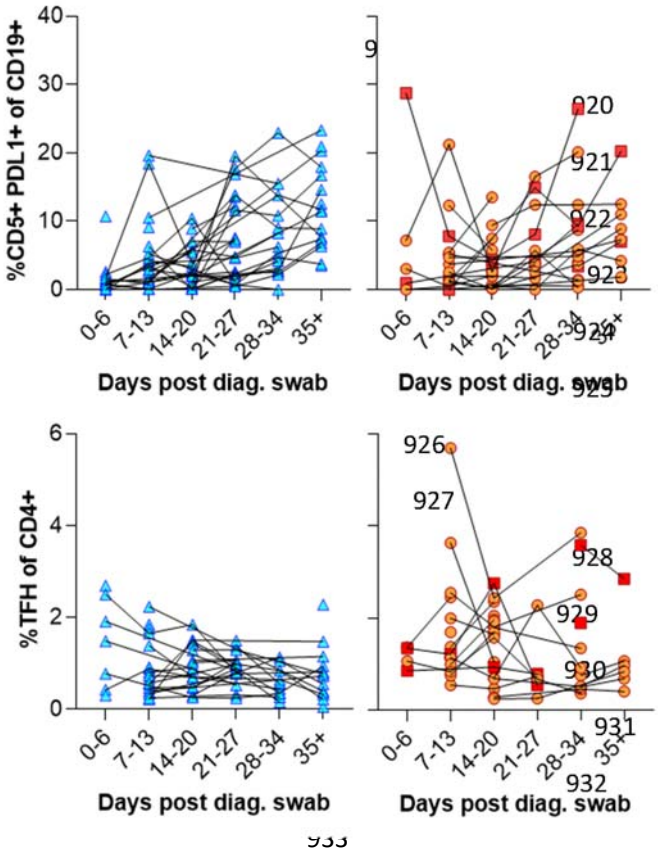

Extended Data Figure 5.